



აჭარის ავტონომიური რესპუბლიკის  
განათლების, კულტურისა და სპორტის სამინისტრო  
MINISTRY OF EDUCATION, CULTURE AND SPORT  
OF AJARA AUTONOMOUS REPUBLIC

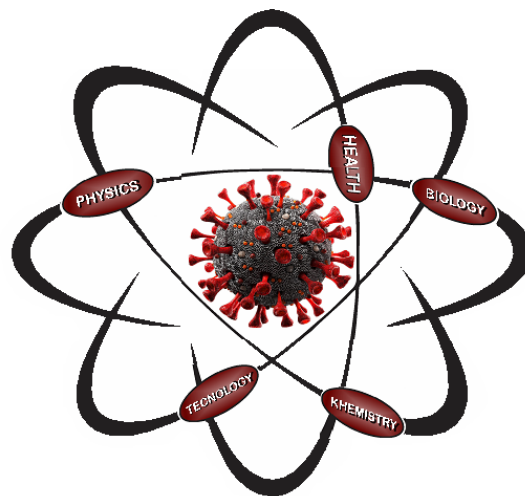


საერთაშორისო სამეცნიერო კონფერენცია  
ბიო-ნანო-აგენტების კვლევის თანამედროვე მეთოდები  
ბათუმი, 24-26 ნოემბერი, 2021

კონფერენციის მასალები

International Scientific Conference  
Modern Research Methods of Bio-Nano-Agents  
Batumi, 24-26 November 2021

Conference Materials



#### TOPICS:

- Study of radiation and spectroscopy methods for research and treatment of bioagents;
- Study simple and effective ways to use sum-frequency generation and other infrared and Raman spectroscopic instruments to measure the physical properties of viruses and other bioparticles.
- Further development of modelling and simulation methods for measuring the effects of vibration in different viruses and other bioparticles.
- Creating a market for researchers and entrepreneurs to introduce new spectrometric methods in practical biomedical activities.
- Elaboration of modern modelling and experimental methods for determining the vesical and vibrational properties of pathogenic microorganisms.
- Elaboration of measuring and therapeutic methods and tools of vibrational parameters of virus-like particles using the developed method in biological laboratories and clinics.

#### INTERNATIONAL ADVISORY COMMITTEE MEMBERS:

- **Paata Kervalishvili** - Georgian Technical University, President of Georgian Academy of Natural Sciences, President of Euro Mediterranean Academy of Arts and Sciences
- **Christophe Humbert** - CNRS Research Director, Université Paris-Saclay
- **Waclaw Gudowski** - professor of Neutron and Reactor Physics at Kungliga Tekniska Högskolan (KTH) and director of the Nuclear Energy Technology Centre The Royal Institute of Technology in Stockholm, Sweden.
- **Jeremy Ramsden** - Chief editor of international scientific magazine Nanotechnology Perceptions, Professor of University of Buckingham
- **Pedro De Oliveira** – Professor of University Paris-Sud, Vice Director of Laboratory of Chemical Physics
- **Laszlo Sajti** - Professor and head of department of Austrian Institute of Technology.
- **Dimitris Tseles** – University of West Attica, Head of Administration of Euro Mediterranean Academy of Arts and Sciences
- **Stane Pejovnik** – Rector of University of Ljubljana, Presidium member of Euro Mediterranean Academy of Arts and Sciences

#### ORGANIZING COMMITTEE:

- **Nugzar Gomidze** – Professor of Batumi Shota Rustaveli State University
- **George Chakhunashvili** – Professor of Tbilisi State Medical University
- **Tamar Berberashvili** – Associated Professor of Georgian Technical University, Manager of International projects
- **Lasha Bazadze** – Director General of K.Eristavi National Center for Surgery
- **Anna Kekelidze** - Biosafety expert of Agriculture State Laboratory
- **Lela Turmanidze** - Professor, Dean of Faculty of Exact Science and Education of Batumi Shota Rustaveli State University
- **Izolda Jabnidze** – Associated Professor of Batumi State University
- **Lali Kalandadze** – Associated Professor of Batumi State University
- **Eldar Mskhaladze** – IT of Batumi State Maritime Academy
- **Miranda Khajishvili** – Dr, Batumi State University
- **Kakha Makharadze** – Dr, Batumi International Hospital



## ბიო-ნანო-აგენტების კვლევის თანამედროვე მეთოდები



საერთაშორისო სამეცნიერო კონფერენცია „ბიონანოაგენტების კვლევის თანამედროვე მეთოდები“ ჩატარდა ბათუმის შოთა რუსთაველის სახელმწიფო უნივერსიტეტის ორგანიზებითა და აჭარის ავტონომიური რესპუბლიკის განათლების, კულტურისა და სპორტის სამინისტროს მხარდაჭერით.

კონფერენციის სამეცნიერო პროგრამის მომზადებაში ბათუმის სახელმწიფო და საქართველოს ტექნიკურ უნივერსიტეტებთან ერთად აქტიური მონაწილეობა მიიღეს მსოფლიო დონის სახელმწიფო, საუნივერსიტეტო და საზოგადოებრივმა სამეცნიერო-კვლევითმა ორგანიზაციებმა, საფრანგეთიდან, დიდი ბრიტანეთიდან, ავსტრიიდან, გერმანიიდან, საბერძნეთიდან, იაპონიიდან და სხვა.

კონფერენციის ერთ-ერთი მთავარი სამეცნიერო მიზანი გახლდათ ინოვაციური გადაწყვეტილებების საფუძველზე ახალი სამეცნიერო-ტექნოლოგიური კვლევების განვითარება ოპტიკურ სპექტრომეტრიაში, ლაზერულსა და მოლეკულურ ფიზიკაში, ასევე

ინფორმაციულ ტექნოლოგიებსა და სისტემებში, ბიოსამედიცინო პრაქტიკაზე ორიენტირებული ახალი ბიოფიზიკური და ბიო-სამედიცინო მეთოდებისა და ხელსაწყოების შექმნისათვის.

ნანოზომის ბიოობიექტების შესწავლა და ვიზრაციული სპექტრომეტრიის ძირითადი კონცეფციისა და ნანობიონაწილაკების თვისებების შეფასების ახალი მეთოდების შემუშავება, პათოგენური მიკროორგანიზმების, განსაკუთრებით ვირუსების, უნიკალური „ანაბეჭდის“ დადგენა, რასაც დიდი მნიშვნელობა ბიომოლეკულების თვისებების გამოვლენის, მაკრო/მიკრო გარემოზე დაკვირვების, სამედიცინო დიაგნოსტიკისა და მკურნალობისათვის, ასევე წარმოადგენდა კონფერენციის ერთ-ერთ სადისკუსიო თემას.

კონფერენციის შედეგები, რომლებიც გამოიხატება პათოგენური ნანობიოსისტემების (მათ შორის ვირუსების) სწრაფად, უშუალოდ და შერჩევითად გამოვლენის შესაძლებლობების შექმნაში, მნიშვნელოვნად იმოქმედებს დიაგნოსტიკისა და მკურნალობის ხარისხზე, კლინიკური გადაწყვეტილებების გაუმჯობესებაზე და მიგვიყვანოს უკეთეს შედეგებამდე ჯანდაცვაში.

ბათუმის კონფერენციის დროს წარმოდგენილი სამეცნიერო და ინოვაციური მიღწევები ხელს შეუწყობს ინტერდისციპლინარულ თანამშრომლობის გაღრმავებას (სამედიცინო ფიზიკა და ბიოფიზიკა, კონდენსირებული გარემოს ფიზიკური კვლევები, ბიოინფორმაციული ტექნოლოგიები). ასევე კვლევისა და ინოვაციური პროდუქტების, ცოდნისა და იდეების გაცვლას კლინიკური გამოყენებიდან კვლევამდე და პირიქით, დააჩქარებს შემუშავებული შემოქმედებითი იდეების, ახალი მეთოდებისა და ინსტრუმენტების ინოვაციურ პროდუქტებად გადაქცევას.

### პაატა კერვალიშვილი

საქართველოს ტექნიკური უნივერსიტეტი, ფიზ.-მათ. მეცნ. დოქტორი, პროფესორი,  
 საქართველოს საბუნებისმეტყველო მეცნიერებათა აკადემიის პრეზიდენტი  
 ევრო-ხმელთაშუაზღვის ხელოვნებისა და მეცნიერების აკადემიის პრეზიდენტი



## Modern Research Methods of Bio-Nano-Agents



The international scientific conference "Modern Methods of Research of Bionanoagents" was organized by Batumi Shota Rustaveli State University with the support of the Ministry of Education, Culture and Sports of the Autonomous Republic of Adjara.

World-class state, university level and public scientific-research organizations from France, Great Britain, Austria, Germany, Greece, Japan and others took an active part in the preparation of the scientific program of the conference together with Batumi State and Georgian Technical Universities.

One of the main scientific goals of the conference was to develop new science and technology research based on innovative solutions in optical spectrometry, laser and molecular physics, as well as information technologies and systems, new biophysical and biomedical methods and tools focused on biomedical practice.

Study of nanoscale bioobjects and development of new methods for elaboration of basic concept of vibration spectrometry and evaluation of properties of nanoparticles, identification of pathogen's, especially viruses' unique "fingerprint", which is of great importance for biomolecule properties, also were an important discussion topics of the conference.

The results of the conference, which show the potential for rapid, direct and selective detection of pathogenic nanobiosystems (including viruses), will significantly affect the quality of diagnosis and treatment, improve clinical decisions, and lead to better outcomes in healthcare.

The scientific and innovative achievements presented during the Batumi Conference will contribute to the deepening of interdisciplinary cooperation (medical physics and biophysics, physical studies of condensed matter, bioinformation technologies). Also, the exchange of research and innovative products, knowledge and ideas from clinical application to research and vice versa, will accelerate the transformation of developed creative ideas, new methods and tools into innovative products.

### **Paata Kervalishvili**

Georgian Technical University, Doct. Phys.-Math. Sci., Professor  
President of Georgian Academy of Natural Sciences,  
President of Euro Mediterranean Academy of Arts and Sciences



## Table of Contents

P. Kervalishvili · Vibrational properties of nanobiparticles and concept of resonance therapy -----	6
T. Berberashvili, P. Kervalishvili. Experimental Methods of Investigation of Vibrational Properties of Nanobioobjects -----	9
P.Kervalishvili li, T.Bzhalava. Application of Resonance Scattering (RS) Method for Simulation Study of Bioagents ---	
-----	13
M.Gigineishvili; M.Chikhladze, T.Khachidze, T.Mikeladze. ·Determining the duration of the sensorimotor reaction -----	15
D.Khachidze, N.Khachidze. Microcalorimeter for diagnostics -----	16
L.Kalandadze, O.Nakashidze, N.Gomidze, I.Jabnidze . Validity of modified Maxwell-Garnett effective-medium Theory in Ferrofluids -----	18
N.Gomidze, J.Shainidze, M.Khajishvili, I.Jabnidze, K.Makharadze, L.Kalandadze, O.Nakashidze, Z,Surmanidze, E. Mskhaladze, L.Gomidze. 3D fluorescence spectroscopy to study the distribution of bioparticles -----	21
C. Humbert · Nonlinear optical spectroscopy of biointerfaces -----	27
L. Sajti Ultrapure Nanosystems for Applied Biomedicine-----	28
A. Kantaros, T. Ganetsos , D. Tseles. 3D Printing and 3D Scanning: Applications in the Cultural Heritage field -----	30



# Vibrational properties of nanoparticles and concept of resonance therapy

P. Kervalishvili

Georgian Technical University (GTU), Georgia  
[paata.kervalishvili@gtu.ge](mailto:paata.kervalishvili@gtu.ge)

**Abstract.** The possibility of vibration always exists wherever there is periodic and repeated movement of a particle about a position of equilibrium or balance. This process is also natural for nanosized bioparticles of enveloped, positive-strand RNA viruses which infect amphibians, birds, and mammals and now known as coronaviruses. Coronaviruses are important human and animal pathogens. In late 2019, the new coronavirus was identified as the cause of a cluster of pneumonia cases in Wuhan, a city in China's Hubei province. It spread quickly, leading to an epidemic across China, followed by an increase in cases in other countries around the world. This study aimed to explore nanobiospectroscopy research and technology in order to provide a theoretical, computer modelling and experimental basis for development of methods and tools of identification of characteristic vibrational frequency of viruses and then their resonance therapy.

## 1. Introduction

Bioparticles, like other biological objects, are characterized not only by systemic biological properties, but also purely physical. Physical parameters can include their mass, speed of movement, mechanical, electrical, magnetic energy, etc. Since the bioobjects like viruses travel much less than the speed of light, are small in size and mass, vibrate with a certain frequency relative to a fixed coordinate system, then it is possible to use as a model a Schrödinger equation.

$$i\hbar \frac{\partial \psi}{\partial t} = -\frac{\hbar^2}{2m} \Delta \psi + V(x, y, z, t) \psi,$$

Where:

$$\Delta \equiv \frac{\partial^2}{\partial x^2} + \frac{\partial^2}{\partial y^2} + \frac{\partial^2}{\partial z^2},$$

is Laplace operator in  $(x, y, z)$  coordinates,  $t$  – time,  $m$  – mass,  $\psi(x, y, z)$  psi function.  $P$  probability =  $\alpha |\psi|^2$  the probability of finding a virus at a point with coordinates  $(x, y, z)$  at time  $t$ .

This model makes it possible to assert that a nano size object is located not only inside a living cell, but at any distance from it. Moreover, the nanobioobject, particularly virus itself, as a physical object, simultaneously possesses both corpuscular and wave properties [1,2].

Using the wave properties of the virus, we can consider the models of information transfer, scattering and diffraction on other physical objects, including the elements of a living cell. Using the elements of quantum mechanics, We can determine some of the wave characteristics of the viruses.

Following the simple estimations of de Broglie wavelength fits into the linear size of the virus. Evaluation of other viruses using this calculation method gives similar results, which makes it possible to assume that the wave properties of viruses are closely related to their geometry.

Thus, apparently, it is possible to use purely wave terms and diffraction methods of calculation for a more complete study of the vital processes of viruses both inside a living cell and outside it.

We assume that by integrating into the genetic apparatus, causing the formation of genetic defects, viruses change the

process of formation and functional activity of cells, which results in the development of various diseases in living organisms.

In comparison with cellular molecules (nano-ensembles) the size of viruses varies from 20 to 300 nanometers. Practically all viruses by the sizes are smaller, than bacteria. However, the largest viruses, for example a virus of cow smallpox, have the same sizes, as well as the smallest bacteria (hlamidiya and rikketsiya) who too are obligate parasites and breed only in living cells [3]. Therefore, as distinctive features of viruses in comparison with other microscopic causative agents of infections the sizes or obligatory parasitism, and features of a structure and unique mechanisms of replication (reproduction themselves) serve not. Viruses are masterpieces of nanoengineering with a basic common architecture that consists of the capsid – a protein shell made up of repeating protein subunits- which packs within it the viral genome Nano-sized biological agents and pathogens such as viruses are known to be responsible for a wide variety of diseases such as flu, AIDS and herpes, and have been used as bioreagents.

Coronaviruses belong to the subfamily Coronavirinae in the family of Coronaviridae and the genome of CoVs is a single-stranded positive-sense RNA which is larger than any other RNA viruses [4]. The nucleocapsid protein (N) formed the capsid outside the genome and the genome is further packed by an envelope which is associated with three structural proteins: membrane protein, spike protein and envelope protein. As a member of coronavirus family, the genome size of SARS-CoV-2 which was sequenced recently is approximately 29.9 kb [5]. SARS-CoV-2 contains four structural proteins (S, E, M, and N) and sixteen non-structural proteins (nsp1–16) [6]. By studying the physical characteristics of the SARS-CoV-2 virus, which are still poorly understood, it was found that it may be vulnerable to ultrasonic vibrations at frequencies that are used in medical diagnostics [7]. The virus envelope quickly degrades at frequencies of 25 and 50 MHz, both in water and air.

A team of researchers from Massachusetts Institute of Technology conducted computer simulations of the new coronavirus and its mechanical responses to vibration based on solid state physics and limited information gathered about the structure of the virus [7]. Since its exact characteristics are not known, the scientists first modelled the behaviour of the sample with different elastic parameters for the shell and for the spikes (Fig.1).

Natural fluctuations in the virus were almost imperceptible. But after a fraction of a millisecond, external vibrations, resonating with the frequency of the natural vibrations of the virus, led to the formation of a dent in the shell, like when a ball hits the ground.

When the vibration amplitude increased, the coronavirus



cracked. At lower frequencies of 25 or 50 MHz, this happened even faster, both in water and air. These frequencies and intensity of vibrations are within the capabilities of medical diagnostic devices[8].

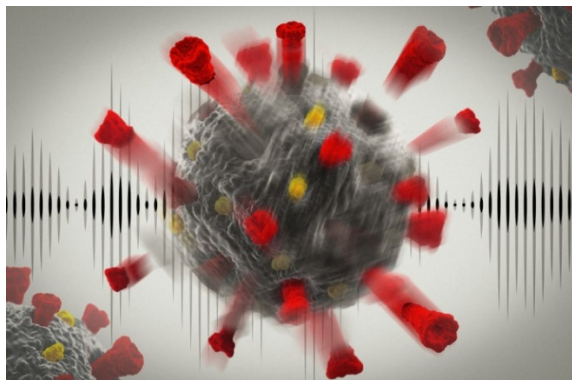


Fig. 1. Ultrasound has potential to damage coronaviruses.  
Credits:Image: MIT News, with images from iStockphoto

## 2. Results of Theoretical and Experimental Investigations

Study of physical properties of viruses, their scattering and absorption characteristics, estimation of electromagnetic (EM) spectrum and resonance wave length ranges are important for determination of biostructures unique spectral signatures, so essential in bio-agents detecting and identification systems. Investigation of EM field distribution makes possible to have insight vision of the nanoparticles. Behavior of nano sized pathogenic microorganisms such as viruses, is selectively sensitive toward the electromagnetic (EM) field excitation. Elaboration of physical models of bioparticles, as well as computer simulation study of near and far EM field distribution in the areas of particles and surrounded medium is a correct way for investigation of physical properties of bioparticles of different morphology.

Method of estimation of spectral response on EM field & particle interaction is based on solutions of electrodynamics two (2D) or three (3D) dimensional boundary tasks [9]. Obtained analytical expressions of EM fields are derived from rigorous solutions of Maxwell's and Helmholtz's equations and defined through the dimensionless parameters, diameters ( $d$ ) over excitation wave-length ( $\lambda$ ). Proposed method was used for investigation of viral particle's physical properties. EM near and far fields distribution, EM spectrum are proposed for viruses, having rod-like, prolate un-enveloped virions (e.g. Tobacco Mosaic Virus (TMV), bacteriophage M13). Virions, the extracellular infective forms of viruses are modelled by the particles of cylindrical shape of different structures, such as homogeneous dielectric particles and inhomogeneous through the radius, also particles of core-shell structure reflecting the properties of ribonucleic acids (DNA or RNA) of viruses and capsid's proteins. Shape, structure and the set of geometrical, magnetic and electrical characteristics are the main parameters defining the particles' EM spectral properties. Advantage of simulation study of complex molecular systems such as virions in contrast of measuring experiments associated with weak signals detection is significant.

Computer simulation (based on MatLabR2013b software) was carried out for TMV particles characterization. Parameters of TMV particle are obtained from scientific publications

based on different measuring technics [10]. Two models are used for simulation study of TMV virion: homogeneous and core-shell structured cylinders. Computer simulation shows that expected resonant spectral response is observable on far-field ( $r \gg (2d_2) / \lambda$ ) characteristics, resonant vibrational frequencies of whole TMV particle may be associated to scattering cross section maximums.

Experimental studies of vibrational parameters of bioobjects were performed by methods of vibrational spectroscopy e.g. Infrared, Ultraviolet, High Resolution Ultrasonic and Raman spectroscopies and Sum Frequency Generation as well [11].

Characteristic group frequencies allow the application of vibrational spectroscopy for structure elucidation. The sensitivity of the vibrational modes for changes in their chemical environment make the different vibrational spectroscopic techniques well suited and widely used analytical techniques.

There are two vibrational spectroscopic techniques (and their variations) to probe the molecular vibrations: IR absorption spectroscopy where the vibrational transitions are directly excited and Raman spectroscopy where the vibrational transitions are probed via an inelastic scattering process.

Molecular vibrations can be excited with radiation in the infrared (IR). If the incident electromagnetic (IR) radiation matches a vibrational transition which involves a change in the electromagnetic dipole moment of the molecule, the molecule gets excited into a higher vibrational level and photons of the matching electromagnetic frequency get absorbed from the incident radiation (Fig.2).

That means a strong change in the electromagnetic transition dipole causes high IR absorption intensity. This is e.g. observed for polar groups such as carbonyl, nitrosyl and hydroxyl groups. Non-polar groups, such as homonuclear diatomic molecules are IR inactive. Each vibrational transition is accompanied by a change in the state of rotation of the molecule. Therefore, the IR absorption spectrum represents a rotational-vibration spectrum.

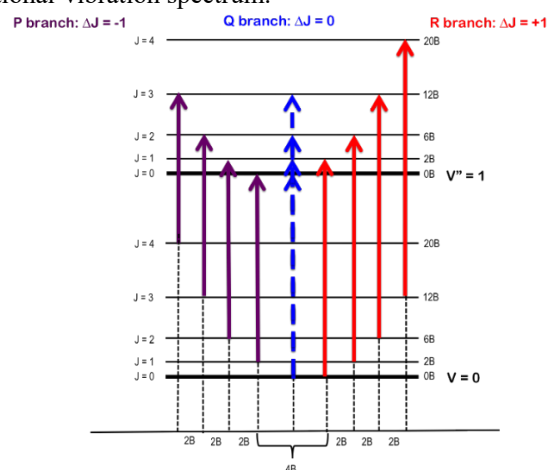


Fig. 2. Cartoon depiction of rotational energy levels,  $J$ , imposed on vibrational energy levels,  $v$ . The transitions between levels that would result in the P- and R-branches are depicted in purple and red, respectively, in addition to the theoretical Q-branch line in blue [12].

Another possibility to obtain high quality Raman spectra bioobjects in solution at low concentration of the substances is resonance Raman spectroscopy. Due to the coupling of the



Raman signal to the electronic absorption high selectivity and sensitivity is obtained and it is possible to record Raman spectra at physiological low concentrations with a good signal-to-noise ratio.

Due to the selective enhancement of the vibrations coupled to the electronic transition (in this case the vibrations of the aromatic ring) changes of the relative intensities of several bands are observed in the resonance Raman spectrum [13]. The vibrational mode most enhanced is the C=C stretching vibration and the ring deformation vibration around 1620  $\text{cm}^{-1}$ . As the enhancement results from a coupling of the vibrational modes (most of the time totally symmetric vibrational modes) to an electronically excited state it is possible to exclusively select vibrational modes by choosing an appropriate wavelength (Fig.3). The off-resonance Raman spectrum excited at 532 nm shows a very complex vibrational structure, since all Raman active vibrations contribute to this spectrum.

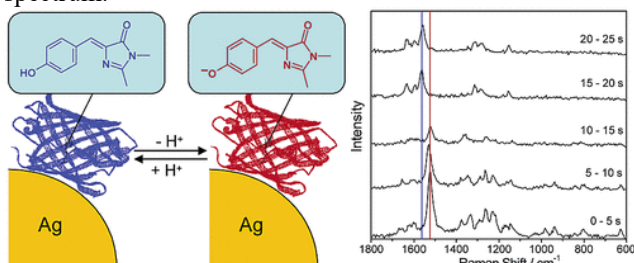


Fig.3. Surface-enhanced resonance Raman scattering spectra from single green fluorescent proteins [13]

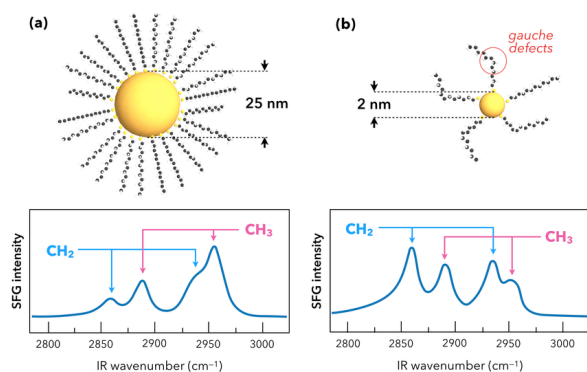


Fig.4. Evolution of the SFG vibrational fingerprint (C-H spectral range) of dodecanethiol molecules (DDT) adsorbed on AuNPs of 2 nm (a) and 25 nm (b) diameter, respectively. [16]

The special attention was paid to nonlinear Two-Color Sum-Frequency Generation Spectroscopy (2C-SFG) that meets the desired spectroscopic requirements [14].

The goal of this approach is to probe membrane models of various forms and in various environments: (i) lipid monolayers and bilayers; (ii) deposited on substrates, floating on water as Langmuir layers and at a liquid-liquid interface; (iii) alone and in interaction with molecules, including peptides and proteins; (iv) submitted to controlled stress (chemical, pH, electrochemical potential). Configuration of SFG experiment in case of thin solid films like a ligand-conjugated CdTe QDs might be described by following main actions: its deposition on a CaF<sub>2</sub> prism and probed by 2C-SFG spectroscopy. The visible, IR and SFG beams belong to the incidence plane (y, z), like their respective polarizations as their frequency is  $\omega_{\text{vis}}$ , excites NCs by creating confined

electron-hole pairs ( $e^-$ ,  $h^+$ ) called excitons, while the IR beam, at frequency  $\omega_{\text{IR}}$ , excites vibration modes of their ligands [15]. The SFG beam is generated as a combination of both, and as a signature of the NC/ligand vibroelectronic coupling. Evolution of the SFG vibrational fingerprint is shown on the fig.4.

We are thinking that biological viruses, have an ability to play at the same time the role of information carriers (information-wave viruses). They should contain encoded information about the object of which they are informational expressions. Each information-wave virus has its own digital code.

Viruses, invading the field envelope of a person, can actively interact with the cells of the body (organs). It is logical to assume that there is a resonant interaction of the wave structure of viruses with those parts of the human genetic apparatus where there are biological chains of viruses.

### Conclusions

Spectroscopic methods have the characteristic of providing fast results and reliable information related to the composition of the samples. The studies presented here have shown promising results in a field of science that needs to be better explored. It has been shown that multivariate analysis techniques are of great importance to analyze spectroscopic data, providing the potential to identify and classify biological samples. We do hope that with advancement in this field of study, spectroscopic methods and tools will be used in bio medicine in the nearest future. Methods of light therapy of different diseases based on estimation of EM field characteristics and resonant wave ranges based on computer simulation of nanobioparticles characterization will be widely implemented, and possibility of determination of resonant (own) frequencies of entire system of molecules including virions will be a key point for that.

It is a well-known fact that the yogis of ancient times practiced meditational techniques to get rid of diseases and stay healthy. Meditations induce the positive vibrations which are known to kill many of the harmful microorganisms which get into our body. Recent frontiers in technology are exploring the possibility of using external excitations to vibrate a virus to its death.

The genetic material of virus is DNA/RNA enclosed within the protective protein shell (Capsid). Every cell in human body has a natural tendency to vibrate at frequency known as the natural frequency, and so the virus. Natural frequency values of these vibrations are very high compared to healthy cells, and depend on the molecular structure and differ from virus to virus [17,18].

In our opinion the concept and relevant methods of resonance therapy will be basis of different viral deceases treatment in the nearest future of practical medicine.

### References

- [1] Kervalishvili P. Entropy of a biosystems. International conference of Euroscience Georgian national section, Tbilisi, 5 June, 2021, Tbilisi state medical university.
- [2] Kervalishvili P. Gotsiridze I. Oscillation and optical properties of viruses and other pathogenic microorganisms, NATO Science and Security series – Physics and Biophysics, Springer, 2016, p 187-196.





- [3] Kervalishvili P., Bzhalava T. Investigations of Spectroscopic Characteristics of Virus-Like Nanobioparticles, American Journal of Condensed Matter Physics v.6. no.1, April, p.7-16, 2016.
- [4] Brian D.A., Baric R.S. Coronavirus genome structure and replication. Review Curr Top Microbiol Immunol. 2005, 287, 1-30. doi:10.1007/3-540-26765-4\_1.
- [5] Wenling Wang, Yanli Xu, Ruqin Gao et al. Detection of SARS-CoV-2 in Different Types of Clinical Specimens. JAMA,2020;323(18):1843-1844. doi:10.1001/jama. 2020.3786.
- [6] Ahmad Abu, Turab Naqvi, Kisa Fatima,Taj Mohammad et all. Insights into SARS-CoV-2 genome, structure, evolution, pathogenesis and therapies: Structural genomics approach. Biochimica et Biophysica Acta (BBA) - Molecular Basis of Disease, Volume 1866, Issue 10, 1 October 2020, 165878.
- [7] Jennifer Chu, Ultrasound has potential to damage coronaviruses, study finds. MIT News Office, Publication Date:March 16, 2021.
- [8] Berberashvili T., Bzhalava T., Chakhvashvili L., Kekelidze A., Karseladze S., Bazadze L., Talebifar T., Soselia A., Kervalishvili P. Investigations of Vibrational Properties of Viruses and Virus-like Particles by Computing Methods Social, Ecological and Clinical Pediatrics, # № 23-18-17, 2021, pp. 25-33.
- [9] Kervalishvili P., Bzhalava T, Computer Simulation Study of Oscillation Mechanisms and Physical Properties of Nanosized Biostructures, Published in book: Innovative Smart Healthcare and Bio-Medical Systems, CRC Press – Taylor and Francis, New York, 2020, Chapter 6, 8 pages. doi <https://doi.org/10.1201/978100304429>.
- [10] Kervalishvili P., Bzhalava T. Computer Simulation Study of Physical Properties of Nanosized Biostructures. 11th Japanese-Mediterranean Workshop on Applied Electromagnetic Engineering for Magnetic, Superconducting Multifunctional and Nanomaterials., Batumi Shota Rustaveli State University July, 16-19, 2019, Batumi, Georgia.
- [11] Kervalishvili P. Study of Vibrational Properties of Viral Particles by Computer Modeling. Egyptian Computer Science Journal Vol. 45 No.2 May 2021, pp 44-65. ISSN-1110-2586.
- [12] Monty L. Fetterolf. Enhanced Intensity Distribution Analysis of the Rotational-Vibrational Spectrum of HCl. J. Chem. Ed. 2007, 84, 1064. DOI: 10.1021/ed084p1062.
- [13] Satoshi Habuchi, Mircea Cotlet, Roel Gronheid, Gunter Dirix et al, Single-Molecule Surface Enhanced Resonance Raman Spectroscopy of the Enhanced Green Fluorescent Protein. J. Am. Chem. Soc. 2003, 125, 28, 8446–8447. <https://doi.org/10.1021/ja035331>.
- [14] Mostafavi M., Tadjeddine A., Humbert C., Kervalishvili P., Bzhalava T., Kvintradze V., Tsirekidze M., Kakabadze G., Berberashvili T. Studying Physical Characteristics of Nano-Bio-Materials for Sensory Applications. International conference advanced materials and technologies, dedicated to the 70th anniversary of foundation of Ilia Vekua Sukhumi Institute of Physics and Technology, Proceedings, Tbilisi, Georgia p.p. 188-192, 2015.
- [15] Noblet T., Dreesen L., Boujday S., Méthivier C., Busson B., Tadjeddine A., Humbert C. Semiconductor quantum dots reveal dipolar coupling from exciton to ligand vibration. Communications Chemistry, 2018. DOI: 10.1038/s42004-018-0079-y.
- [16] Christophe Humbert, Thomas Noblet, Laetitia Dalstein, Bertrand Busson, Grégory Barbillon. Sum-Frequency Generation Spectroscopy of Plasmonic Nanomaterials: A Review Materials (Basel), 2019 Mar 12;12(5):836. doi: 10.3390/ma12050836.
- [17] Bruno Roberts. Resonance Raman spectroscopy. Photosynthesis Research volume 101, 2009, pages147–155.
- [18] Kervalishvili P. Concept of Study of Vibrational Properties of Viral Particles; Spectroscopic methods of nanobiosystems investigation: detection of viruses and resonance therapy. Austrian – Georgian Workshop “New of Applied Physics for Nanobiomedicine”.TFZ Technologie- und Forschungszentrum Wiener Neustadt, Wien, Austria, October 21, 2021.

## Experimental Methods of Investigation of Vibrational Properties of Nanobiobjects

T. Berberashvili, P. Kervalishvili

Georgian Technical University (GTU)

[t.berberashvili@gtu.ge](mailto:t.berberashvili@gtu.ge) [paata.kervalishvili@gtu.ge](mailto:paata.kervalishvili@gtu.ge)

**Abstract:** Diseases caused by viral infections are one of the biggest problems for global health, and as methods involved in diagnostics are getting faster and more efficient, methods of their therapy are still need to be stronger. Our studies aimed to explore nanobiospectroscopy research and technology in the field of virology in order to provide a theoretical, computer modeling and experimental support for the techniques used, and to suggest the applying tools that have not been used previously.

### 1. Introduction

Viruses are assembled in the infected host cells of human, animals, or plants.(Fig.1). Because of viral breeding the, host cell dies. There are especially viruses which are breeding in the cell of the bacteria. Viruses spread in many different ways. Just as many viruses are very specific as to which host species or tissue they attack, each species of virus relies on a particular propagation way [1].

The interdisciplinary collaboration (Biomedicine and Biophysics, Physical Research, Information Technologies and Systems) is an engine of strengthen the abilities of researchers in development of new biophysical and biomedical methods and tools. Those works which are based on novel achievements in optical spectrometry, laser and molecular

physics as well as information technologies and systems are critically important for study of common properties of nano-scale virus-like particles, and elaboration of basic concepts and new revolutionary method for estimation unique vibration/oscillation properties, determine the unique “fingerprints” of pathogenic micro-organisms, especially viruses.

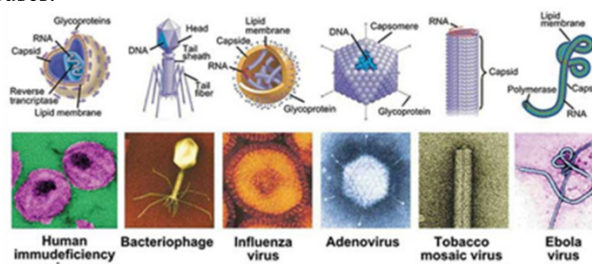


Fig.1 Virus Classification on the basis of morphology and replication, by Somak Banerjee, 2021 [2]

During the past two decades methods of vibrational spectroscopy have become valuable tools for the study of



structural properties and dynamical processes of biomolecules and particularly bionanoparticles and their clusters. (Fig.2) Farther development of new methods of pathogens treatment is greatly facilitated by an improved understanding of epidemic diseases. There is therefore a need to address the current knowledge gaps in disease aetiology in order to support innovation in evidence-based therapy. In this context, a better understanding of the mechanisms that are common to several diseases, in particular of those leading to co-morbidities, constitutes an important challenge. Performing activities should assess and validate the relevance of these common mechanisms and of their biomarkers (where relevant) on the development of co-morbidities in both males and females [3].

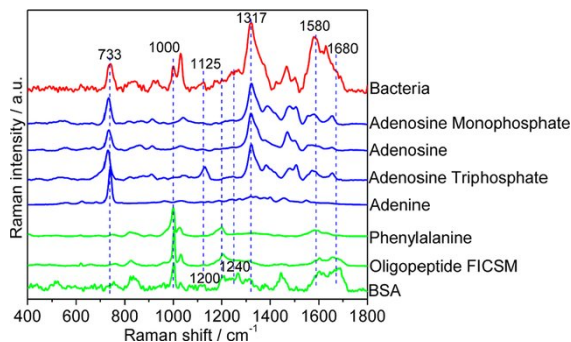


Fig.2. SERS spectra of biomolecules as reference for band assignments [4]

Behavior of nano-micro sized pathogenic microorganisms such as bacteria, virus, organic and non-organic agents is selectively sensitive toward the electromagnetic (EM) field excitation. Elaboration of physical model of structural behaviour of bionanoparticles, as well as computer simulation study of near and far EM field distribution in the areas of particles oscillation and surrounded medium is a possible way for investigation of physical properties of bionanoparticles of different morphology [5].

In this direction the multidisciplinary development of ability to detect rapidly, directly and selectively individual virus particles has the potential to significantly impact healthcare, since it could enable diagnosis at the earliest stages of replication within a host's system. Simultaneous acquisition of the vibrational and electronic fingerprints of molecular systems of biological interest, at the interface between liquid media, or at the air/solid, air/liquid interfaces is difficult to achieve with conventional linear optical spectroscopy due to their rather poor sensitivity to the low number of molecules or their maladjustment to water environment (infrared absorption). It relies on inelastic scattering of monochromatic light, usually from a laser in the visible, near infrared, or near ultraviolet range. The laser light interacts with molecular vibrations, phonons or other excitations in the system, resulting in the energy of the laser photons being shifted up or down. The shift in energy gives information about the vibrational modes in the system. Infrared spectroscopy yields similar, but complementary, information. Spontaneous scattering is typically very weak, and as a result the main difficulty of this kind of spectroscopy is separating the weak non-elastically scattered light from the intense Rayleigh scattered laser light. With the advancement of technology and

consequently advanced spectroscopy, the interest of researchers in spectroscopic techniques in biological studies has grown. This field of science is known as biospectroscopy, and means the use of spectroscopy to analyze biological objects. Several studies have been conducted involving identification of bacteria, viruses, cancer diagnosis, and even in the field of forensic entomotoxicology, demonstrating that spectroscopic techniques are capable of detecting biochemical changes in biological matrices. Viruses are submicroscopic infectious agents and obligate intracellular parasites. They are totally dependent on a host cell because they are not able to generate energy to conduct all biological processes. Virus particles (virions) come in a variety of sizes and shapes.

## 2. Results and Discussion

However, approximately spherical shapes with diameters in the range between 50nm and 100nm are especially common. Many nearly spherical viruses are revealed by X-ray crystallography to have icosahedral symmetry. A typical virus particle contains genetic material, RNA or DNA, surrounded by a protein coat (capsid). Such an object should have reasonably distinct vibrational frequencies, the study of which may be of interest. Excitation of these vibrations could have applications in either the diagnosis or treatment of viral diseases. The sole discussion of these vibrational modes conjectured that ultrasound in the GHz range could be resonantly absorbed by HIV virus particles, leading to their destruction.

The two methods most commonly used in clinical diagnoses of viruses are enzyme-linked immunosorbent assay, with the best known being the ELISA method and real-time polymerase chain reaction (PCR). These methods have brought benefits such as high levels of repeatability and reproducibility, ease in handling and robustness. However, they have also some negative points. As example, both methods requires high quality reagents; in some situations they are not suitable for identifying specific viral species/strains and they are also destructive to the samples. Thus, there is a need for techniques that are as advantageous as ELISA and PCR techniques, and which have fewer disadvantages.

An expected difficulty in the use of biospectroscopy in virology is related to the fact that humans have a great diversity of virus circulating in their organism, and each human has a unique microbiome. Because of it, obtaining a fingerprint would be more difficult in view of the specificity of each organism. The solution to this problem seems to be the use of a broad and well-trained database, and changes obtained by multivariate statistical analysis, differentiating these alterations. The main spectroscopic techniques that have been used in virological studies are nuclear magnetic resonance spectroscopy (NMR), Raman spectroscopy, infrared spectroscopy (IR) and molecular fluorescence spectroscopy. These techniques are known to provide rapid responses and reliable data, as well as having powerful structural elucidation capability [7]. Such advantages highlight the possibility of identifying and classifying different types of virus using spectroscopic techniques. In this paper, studies using biospectroscopy coupled to statistical methods of classification in virological investigations are emphasized. First, we will discuss the most commonly used spectroscopic



techniques, and then we will discuss the computational processes used to extract useful information from the obtained spectra (spectral preprocessing, multivariate classification algorithms, performance evaluation). The potential of spectroscopic techniques in the detection and identification of virus-infected cells has been studied using statistical methods as a sensitive, rapid and reliable methodology. The ability to discriminate between contaminated and non-contaminated objects in a short time with high sensitivity which characterized biospectroscopy determine its high prospect for studying viruses and similar pathogens [8].

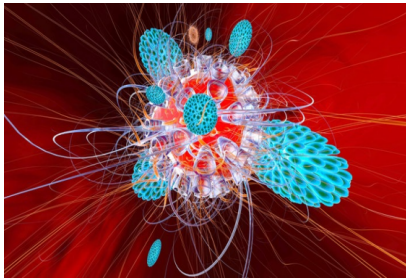


**Fig.3. ELISA (Enzyme-Linked Immunosorbent Assay)** Once the immune system has developed antibodies against an antigen, it can react quickly to later infections. Then the defense cells (here in blue) attack the virus [6]

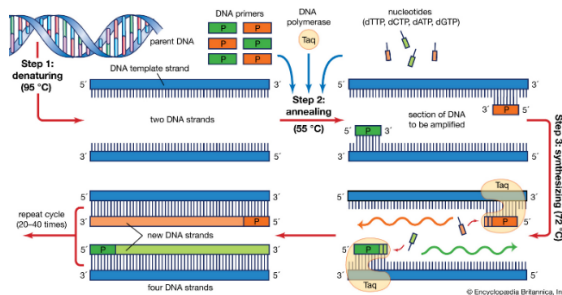


**Fig.4. The three-step process of the polymerase chain reaction-PCR.** Encyclopædia Britannica, Inc.

Molecular fluorescence spectroscopy is based on effect of excess energy by excited species and its main advantage is inherent sensitivity, which is often one of three orders of magnitude better than in case of absorption spectroscopy. Although molecular fluorescence spectroscopy has been little used in studies in the field of virology, it is also an interesting approach with great potential in this perspective. This technique analyzes the fluorescence capacity of a sample, where a beam of high energy light (usually in the ultraviolet region) is irradiated on the sample to be excited into a higher electronic energy level; then the fluorophore molecule will rapidly lose energy to this environment through non-radiative modes (called internal conversion) and will return to the lowest vibrational level of the lowest electronic excited state. The molecule persists at this vibronic level for a period of time known as the fluorescence lifetime, and then returns to the fundamental electronic state by emitting a photon with energy lower than the irradiated one [12].

The excitation and emission spectrum are recorded by the instrument and is generally used to build excitation-emission (EEM) fluorescence matrices. Another commonly-employed form of fluorescence technique is fluorescence correlation spectroscopy (FCS), which is used for temporal and spatial

analysis of molecular interactions of biomolecules present in solution at extremely low concentrations. This technique is based on the principle that a fluorophore molecule has a specific free diffusion rate that is directly related to its size. This basic principle, for example, can be used to study protein interactions. As with other spectroscopic techniques, molecular fluorescence spectroscopy provides rapid results with high sensitivity and specificity, and is non-destructive, making this technique a tool of interest in the field of virology.

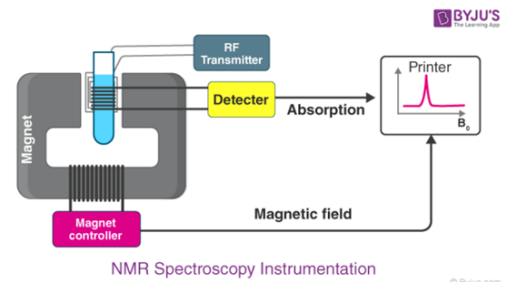


**Fig.5. Scheme of method of Nuclear Magnetic Resonance Spectroscopy. (NMR)**

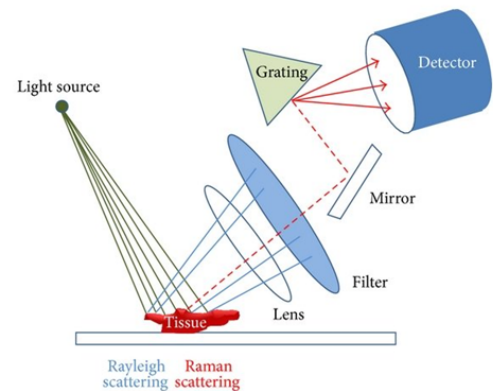


**Fig.6. Schematic presentation of Raman spectroscopy**

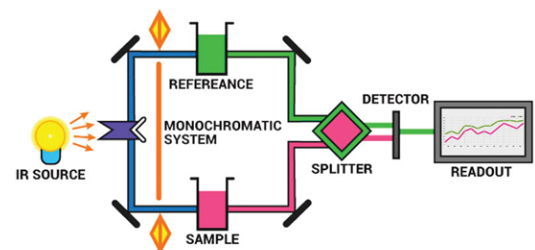


**Fig.7. Infrared (IR) Spectroscopy – Instrumentation**

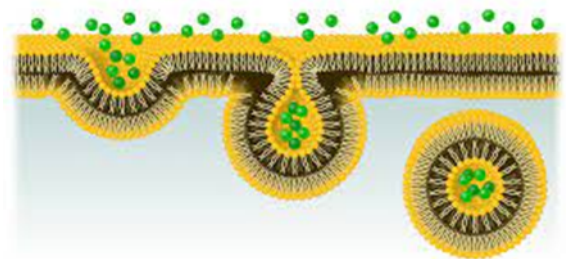


**Fig.8. Endocytosis and Exocytosis**

### 3. Instead of Conclusion.

In order to understand the possible pathway of



biospectroscopy development it is necessary to use the new science and technology tool calls bionanotechnology. The main objective of this modern discipline is cellular uptake of nanosize molecules functioning within the cell. If the size of molecules is bigger than 10nm are taken by the cell through a clathrin-assisted mode of endocytosis called pinocytosis, while particles of size greater than 200 nm in diameter are usually phagocytosed by the macrophages. Phagocytosis occurs in specialized cells called phagocytes, which includes macrophages, neutrophils, and other white blood cells, which destroys the molecular association. Invagination produces so called phagosome which usually fuses with one or more lysosomes containing hydrolytic enzymes [9].

One of the most promising methods of biospectroscopy is SFG. These ultrashort pulsed lasers based optical measurement method is unique for investigation of vibrational modes of different viruses and other pathogenic microorganisms as well as study of nature of their oscillation processes and parameters of oscillation. Non-linear optics and its resonance technologies is possible direction of organization of treatment of pathogenic microorganisms in their different living media. Contrary to the previous ones, this second order nonlinear process is intrinsically specific to an interface, and involves no contribution from molecules in a centrosymmetric bulk, i.e., in solution or in gas phase. It has been extensively applied to solid interfaces in vacuum, controlled atmosphere and electrochemical conditions. For a few years, technological development of picosecond and femtosecond tunable laser sources have led both to an increase of the number of SFG experimental setups around the world and to a progressive application to fragile or buried interfaces. In addition to unique SFG setup is research based on usage of the CLIO Free Electron laser. This latter allows probing specific vibrations located in the near and far infrared, which is again unique to date [10].

Spectroscopic methods have the characteristic of providing fast results and reliable information related to the composition of the samples. The studies presented here have shown promising results in a field of science that needs to be better explored. We do hope that with advancement in this field of study, spectroscopic methods and tools will be used in biomedicine in the near future. Methods of light therapy of different diseases based on nanoparticle characterization

will be widely implemented, and possibility of determination of resonant (own) frequencies of entire system of molecules including virions will be a key point for that.

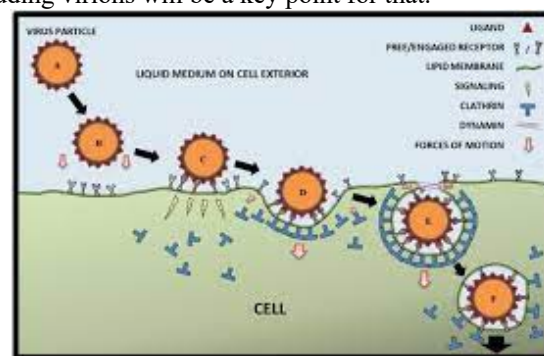


Fig.9. (A) Virus approaches the cell surface. (B) Biochemical interactions between ligands and receptors attract virus to the cell surface. (C) Virus attaches to the cell surface and signals the cell. (D) A clathrin-coated pit is formed around the bound virus. (E) A clathrin-coated vesicle is formed, and the dynamin at the neck region facilitates vesicle scission. (F) The vesicle travels to cell interior

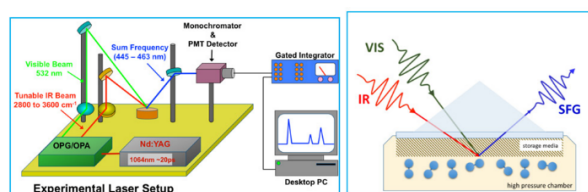
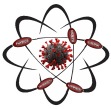


Fig.10. Sum Frequency Generation Vibrational Spectroscopy [11]

## References

- [1] Kervalishvili P., Gotsiridze I. Oscillation and optical properties of viruses and other pathogenic microorganisms, NATO Science and Security series – Physics and Biophysics, Springer, 2016, p 187-196.
- [2] <https://thebiologynotes.com/virus-classification-on-the-basis-of-morphology-and-replication/>.
- [3] Kervalishvili P., Bzhalava T., Berberashvili T., Chakhvashvili L. Spectroscopic methods of nanobiosystems investigation: detection of viruses and resonance therapy, International conference of Euroscience Georgian national section, Tbilisi, 20 December, 2020, Tbilisi state medical university.
- [4] Li Cui, Yingjiao Zhang, Wei E Huang, Bi-Feng Zhang Surface-enhanced Raman spectroscopy identifies heavy metal arsenic(V)-mediated enhancing effect on antibiotic resistance. Article in Analytical Chemistry February 2016 DOI: 10.1021/acs.analchem.5b04490



# Application of Resonance Scattering (RS) Method for Simulation Study of Bioagents

P. Kervalishvili<sup>a</sup>, T. Bzhalava<sup>b</sup>

Georgian Technical University (GTU), Georgia

<sup>a</sup> [kerval@global-erty.net](mailto:kerval@global-erty.net), <sup>b</sup> [tamar.bzhalava@gtu.ge](mailto:tamar.bzhalava@gtu.ge)

**Abstract:** Resonance scattering method (RS) elaborated on the basis of classical Maxwell's electromagnetic (EM) theory is proposed for simulation study of physical properties of harmful agents of different origin in purpose of elaboration of basis of identification systems and technologies. Well-known physical tasks of EM field & particle interaction, models of nano- and micro-sized particles, solution of corresponding electrodynamics two (2D) and three (3D) dimensional boundary problems are considered. Based on separation of variables method, solution of Helmholtz's equations makes possible to define EM fields in different areas of particles as the sums of multipole waves and estimate the scattering ability of particles as well as the field distribution in near and far zones of the particles. The elaborated models are based on morphology and structure of bio-agents. Analytical mathematical models are used for simulation study of bio-agents scattering and resonance properties. Software and graphical user interface are elaborated for a case of single spherical virus-like particles (VLPs). Numerical results are given for VLP of T7 virions. Resonance wavelengths are observed in ultraviolet (UV) range and depends on VLPs parameters.

## 1. Introduction

Bio-agents of various structure, shape and origin are the object of many research works aimed on improvement of methods and tools for healthcare, biomedical, biosecurity, military, agriculture safety and other purposes. Study of physical properties of bio-structured materials as well as bio-particles became essential for elaboration of modern biomedical sensory or drug-delivery, detecting or identification systems. Estimation of physical, especially optical (scattering or absorption) characteristics describing the behavior of particles in radiated electromagnetic (EM) field, formed by polarized plane waves or pulsed lasers, response on EM & particle interaction is the goal of presented paper.

Characterization of harmful agent nature made and artificial, chemical and biological, micro and nano-sized is quite difficult, requires research based on multidisciplinary knowledge of variety of chemical bonds, physical structures and compositions of complex molecules, sizes overlapping in air, water and other environments. One of the ways of pathing and simplifying the complexity of problem is the use of modern modelling and simulation (M&S) methods based on classical or semi-classical approaches. Based on main concept developed in [1], Resonance Scattering (RS) method comprehends the elaboration of physical models relevant to agents' structure, solving corresponding electrodynamics boundary problems, defining the scattering and absorption fields and characteristics. RS method proposed for consideration is applied to characterization of virus-like particles (VLPs), virions, the extra cellular forms of viruses.

## 2. Method and approach

Resonance scattering method (RS) is elaborated on the basis of classical Maxwell's electromagnetic (EM) theory. Well-known physical tasks of EM field & single particle interaction as well as solution of electrodynamics two (2D) or three (3D) dimensional boundary problems [2-4] applied to VL particles, virions. According on morphology of virions,

each is modelled by the particle (VLP) of cylindrical or spherical shapes. Two different models VLP are considered: a) homogeneous dielectric, b) core-shell structured dielectric reflecting the electric and magnetic properties of ribonucleic acids (DNA or RNA) of viruses and capsid's proteins.

Based on separation of variables method, solution of Helmholtz's equations makes possible to define EM fields in different areas of particles as the sums of multipole waves. Deterministic mathematical model based on exact solution of electrodynamics and corresponding mathematical equations.

Analytical expressions of EM field components, near and far-field characteristics are defined through the dimensionless parameters, diameters ( $d$ ) of particles over excitation wavelength ( $\lambda$ ). It makes possible to expand the well-established solutions of classical models to sub-micro particles characterization.

It is known that micro and nano-bioorganisms such as bacteria, virus, organic agents are selectively sensitive toward the electromagnetic (EM) field excitation, and is clearly observable in resonance frequency ranges. The measurable and the best "seeable" by detectors are the scattering signals. Therefore, for estimation of response on EM wave-VLP interaction, associated with scattering and absorption ability of particle are used the quantities such as scattering cross-sections (Forward, Backward, Total), which correlate with energy density of scattered field across the surface and defined by time-averaged Poynting vectors estimated in far-field of EM components [3]. Modelling "spectra", wavelength dependence of scattering cross-sections may be used as specific, unique spectral signatures of a given VLPs.

RS method based simulation study of scattering characteristics and estimation of resonance wavelength ranges is considered for icosahedral nano-sized virions (T7, Rhino and etc.) modelled by spherical VL particle.

Shape, structure and the set of geometrical, magnetic and electrical characteristics used as the main parameters defining the particles' EM spectral properties. Advantage of simulation study of complex molecular systems such as virions in contrast of measuring experiments associated with weak signals detection is noteworthy.

## 3. Results

Numerical results based on modelling and simulation (M&S) method (using MatLabR2013b software) was carried out for T7 particles characterization. Parameters of T7 virus-particle obtained by means of different measuring technics [5-7]: outer and inner diameters of T7 capsid are  $d_2 = 56.6$  nm and  $d_1 = 42.6$  nm, correspondingly. Dielectric permittivities and magnetic permeabilities are denoted by the symbols:  $\epsilon_1$ ,  $\mu_1$  for core (dsDNA),  $\epsilon_2$ ,  $\mu_2$  - shell,  $\epsilon_3$ ,  $\mu_3$  - surrounded medium. Two models are used for simulation study of T7 virion: homogeneous and core-shell structured of spherically shaped. Based on analysis of VLP models, core-shell model is



preferable if a large portion ( $> 0.6$ ) of volume in virion is occupied by a capsid of proteins ( $V_{caps} \gg V_{core}$ ). Computer simulation shows that resonant vibrational frequencies of whole T7 particle may be associated to scattering cross section maximums, expected resonant spectral response is observable on far-field ( $r \gg 2d^2/\lambda$ ) characteristics (Fig.1). Slight change of dielectric or magnetic parameters core (or shell) makes the shift of maximums toward the longer wave length (upper Fig.1). The effect of absorption in the area of core (green line on Fig.1) is notable, the values of maximums are lowered as expected.

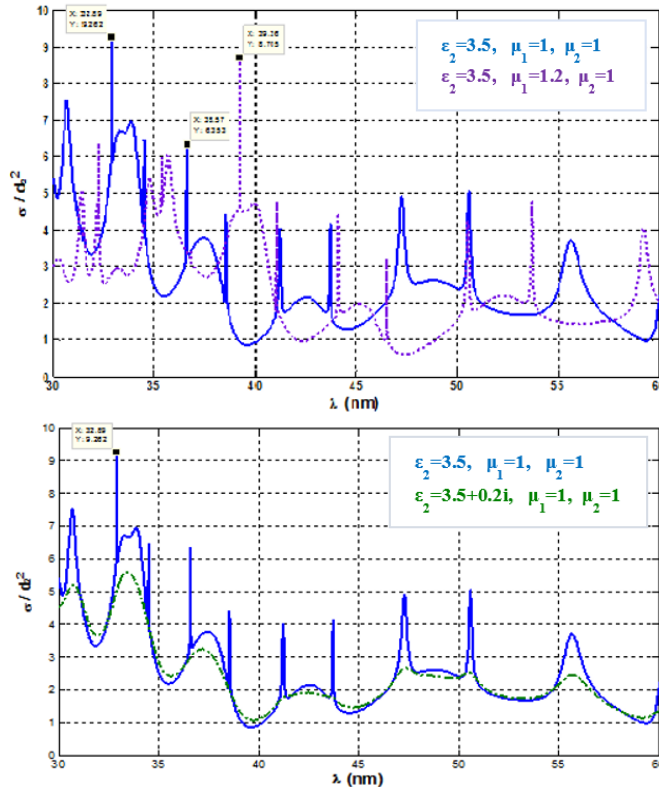


Fig. 1. Forward Scattering Cross Section ( $\sigma_F / d^2$ ) vs excitation wave length ( $\lambda$ ). Spherical core-shell model; outer diameter of shell  $d_2 = 56.6$  nm, inner diameter of shell  $d_1 = 42.6$  nm, dielectric permittivities: of core  $\epsilon_1 = 8$ , surrounding medium  $\epsilon_3 = 1$ , magnetic permeability surrounding medium  $\mu_3 = 1$ .

## Conclusions

Resonance scattering (RS) method based computer simulation is used to study EM field characteristics vs excitation wave length, for estimation of scattering characteristics and defining the resonant wave length ranges correlating with scattering efficiency of VLP, T7 virion. Resonance wavelength range of nano-sized VLP is observed in UV-region, upper theoretical limit depends on VLPs parameters and may be defined by the formula  $\lambda_{max} < \sqrt{\epsilon_q \mu_q} \pi d$ . Analysis of numerical experiments and simulation study revealed the strong dependence of EM field characteristics on electromagnetic and geometrical parameters in resonant wave length range. Simulated EM spectra of given parameters of VLPs are proposed as the specific signatures of virions under consideration. Elaborated Resonance Scattering method is applicable for any nano- and micro scaled particle-like bio or non-bio-agents.

## Acknowledgements

The work was carried out in Georgian Technical University supported by Shota Rustaveli National Science Foundation (SRNSF) under Grant Agreements Carys -19-297.

## References

- [1] Kervalishvili P.J., Bzhalava T.N. Investigations of Spectroscopic Characteristics of Virus-Like Nanoparticles, 2016, American Journal of Condensed Matter Physics, v.6. no.1.
- [2] Bohren C.F., Huffman D.R. Absorption and scattering of light by small particles, 1983, John Wiley & Sons, 530 p.
- [3] Kervalishvili P.J., Bzhalava T.N., Spectroscopy of Bioparticles, 2017, Book, Ed. GTU, Tbilisi, ISBN 978-9941-0-9797-3, pp. 1-244 (in Georgian).
- [4] Bzhalava T.N., Kervalishvili P.J., Study of spectroscopic properties of nanosized particles of core-shell morphology, J. Phys., Conf. Ser. (IOP), 2018, 987, 012023, 1-6.
- [5] Fumagalli L., Esteban-Ferrer D., Cuervo A., Carrascosa J.L., Gomila G. Label-free identification of single dielectric nanoparticles and viruses with ultraweak polarization forces, 2012, Nature Materials, 11, pp. 808–816, doi:10.1038/nmat3369.
- [6] Cuervo A, Dans PD, Carrascosa JL, Orozco M, Gomila G, Fumagalli L. Direct measurement of the dielectric polarization properties of DNA, 2014, Proc Natl Acad Sci USA, 111 (35) E3624-E3630
- [7] Pitera J.W., Falta M., van Gunsteren W.F., Dielectric Properties of Proteins from Simulation: The Effects of Solvent, Ligands, pH, and Temperature, 2001, Biophysical Journal, Vol. 80, pp. 2546–2555.



# Determining the duration of the sensorimotor reaction

M. Gigineishvili<sup>1,2a</sup>; M. Chikhladze<sup>1b</sup>; T. Khachidze<sup>1</sup>, T. Mikeladze<sup>2d</sup>

<sup>1</sup> Georgian Technical University (GTU), Georgia

<sup>2</sup> Clinic "Curatio" Georgia

<sup>a</sup> [m.gigineishvili@yahoo.com](mailto:m.gigineishvili@yahoo.com), <sup>b</sup> [chixladze\\_manana51@mail.ru](mailto:chixladze_manana51@mail.ru), <sup>c</sup> [txachidze@gmail.com](mailto:txachidze@gmail.com), <sup>d</sup> [teimurazmikeladze@yahoo.com](mailto:teimurazmikeladze@yahoo.com)

**Abstract.** The report explains the essence and types of a biological object's sensorimotor reaction. There is given a method for determining the duration of a complex sensorimotor reaction developed in the training laboratory of a Technical University. An electrical scheme of the experiment is presented.

## 1. Introduction

The attempt to cognize one's inner world according to human behavior has a very long history. The speed and accuracy of a person's response to an external signal (stimulus) is his first psychomotor characteristic. Since the human sensorimotor response (response to an irritant) to this or that signal is an integral part of almost any work activity, so the study of the duration and accuracy of this reaction is fundamentally important in terms of solving many everyday problems. In this situation, the sensorimotor reaction develops as a process of interaction between the various functional systems that perceive the real situation and react to it. The scheme of this process can be presented like this:

- The effect of a stimulus on the receptor, which leads to the formation of a nerve signal.
- Transmission of neural signal to the sensitive centers of the analyzer.
- Assess the situation and make a decision.
- Transmitting commands to the cerebral cortex's motor centers.
- Nerve signals transmission to muscles;
- The result of the whole process - the reaction itself.

As we know, biological object has five basic senses for perceiving environment and navigating into it: sight, hearing, smell, taste, and tactile sensation. The sense organs consist of receptors, a nerve conductor and its representation in the cerebral cortex. Each sensory organ gives only the characteristic sensation. However, while acting on the sense organs, the biological object is characterized by a sensorimotor response to the stimulus [1].

Sensorimotor reactions are divided into two types: simple and complex. A simple reaction is when a person knows in advance of the type of sudden impact - the signal (light, sound) and the response. A complex reaction is when the signals and the corresponding response actions are known but the sequence of signals is not known. The complex reaction time is significantly longer than the simple reaction time. It depends on the experience, the prior knowledge of the danger, the mood. It increases according to illness, drug (medicines) use, alcohol intake, abrupt changes in atmospheric pressure and temperature, fatigue, age, and so on [2].

Sensorimotor reactions are characterized by correct action, accuracy, timeliness. The response may be correct but late, or incorrect but timely. Generally, the reaction time increases with age, but experience and the ability to predict the situation compensate slow reaction.

It is obvious that the sensorimotor reaction time depends on both- the condition of the individual functional systems as well as the external conditions that determine the operating parameters of the functional systems. Taking these conditions into account- performing an experiment allows us to obtain data on the dependence of various factors on the reaction time (e.g., the strength of the stimulus signal, the logical complexity of the task, the difficulty of performing the motor reaction, etc.).

The duration of each sensorimotor reaction is divided into two parts: latent (incubation) and motor period.

The latency period is the time interval from the beginning of any irritating action on a biological object to the response. It consists of the following intervals: transmission of nerve impulses from the corresponding receptors to the corresponding area of the cerebral cortex, information processing by the central nervous system, decision-making of the response, transmission of commands to the executing organs. The average latency period of a simple reaction while exposed to light is  $0.3 \div 0.4$  s, in the case of an audible signal  $0.15 \div 0.20$  s. The dynamics of the nervous system can be judged by the length of the latent period.

The motor period is the duration of the response action. It also consists of intervals: stimulating the corresponding muscles, overcoming their inertia, and performing matching actions. The motor period is usually longer than the latent period.

## 2. Method and approach

The characteristics of a person's sensorimotor response give an idea of the real resources and reserves of his personality. Majority of the very different construction tools used to measure the duration of a human sensorimotor reaction are based on measuring the time parameters of the capacitor charging-discharge process at a known impedance. Our goal was - students to be able to determine the time of a complex sensorimotor response under laboratory conditions. In particular, while receiving light signals, they had to perform a response action (eg, by switching off the signal to stop the action and measure the duration of the process) [3].

An electrical scheme shown in the Fig.1 was developed to measure the duration of a complex sensorimotor reaction. In front of a student there are three lamps with different colored lights. The lamps are lit in a different sequence, which is unknown to student, and he has to press his finger as quickly as possible to the corresponding (appropriate) button of the lit lamp.



### 3. Results

The main element of a given electrical scheme is the reaction time counter (TIMER). To turn on the timer, there are key switches K1.1, K1.2, K1.3, (examiners buttons) with each of the two pairs of contacts. By turning them on (the upper pair of contacts on the scheme), a circuit D1.1 (either D2.1 or D3.1, depending on which button examiner chooses) is connected via a semiconductor diode and a releasing signal is supplied to the timer. The device (TIMER) starts counting the time to the nearest hundredth of a second. The second pair of contacts of the examiner's switch (below the diagram) is connected at the same time and the voltage is supplied to the LED (L1), L2, or L3 lamp. One of the lamps (LED) lights up instantly. The speed of this type of light is much faster than the speed of incandescent and gas discharge lamps, which is important for the accurate operation of the device. Therefore, the timing starts and the LED light turns on at the same time. In order to stop the time counting process, we need to remove the first one from the time counting device and deliver the second signal.

To do this, there are buttons - K2.1, K2.2, K2.3 in our scheme. From these three, student should select the button according to the appropriate color of the light bulb and press the finger as fast as possible. Pressing this button disconnects the corresponding contact with the diode D1.1 (or D2.1 or D3.1) and terminates the signal supplied to the timekeeping device, but immediately contacts the diode D1.2 (or D2.2 or D3.2) by which the second signal is already supplied to the time-recording device. The time count stops and the device shows duration of the sensorimotor reaction.

### Conclusions

The duration of the human sensorimotor reaction, especially in the motor part, is natural (congenital) and changes slightly with training. It gradually weakens from adulthood. The length of the motor period plays a key role in professions (eg pilot, instructor, driver, operator, etc.) which is

particularly focused on making quick and correct decisions.

The method we proposed for determining the time of complex sensorimotor reaction is characterized by high accuracy (0,01 sec) and is technically easy to do. At the same time, research can be conducted at minimal cost, which is a prerequisite for its widespread use, both in the teaching process for students and in the relevant field.

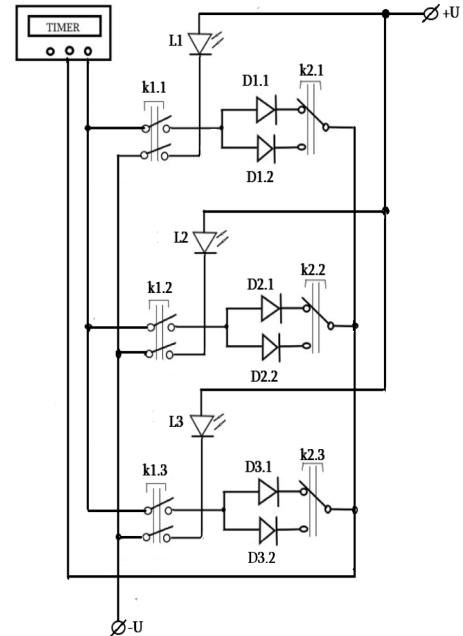


Fig. 1.

### References

- [1] Sidorov P.I; Parniakov A.B; "Introduction of Clinical Psychology". Academic project. Yekaterinburg,2000-416.
- [2] Uznadze D. "General Psychology" e-book Tbilisi 2000.
- [3] Chikhladze M., Giginishvili M., Ketiladze O."The Basics of Medical Physics" Technical University, ISBN 978-9941-20-998-7 (PDF) CD4522, 2018.

## Microcalorimeter for diagnostics

D. Khachidze<sup>1a</sup>, N. Khachidze<sup>2b</sup>

<sup>1</sup>Tbilisi State University (TSU), Georgia

<sup>2</sup>Richard Lugar Center for Public Health Research, Georgia

<sup>a</sup> [davit.khachidze@tsu.ge](mailto:davit.khachidze@tsu.ge) , <sup>b</sup> [nikakhacidze@yahoo.com](mailto:nikakhacidze@yahoo.com)

**Abstract:** It was established that albumin of donor blood serum denatures in two temperature ranges. It is shown that the first stage of denaturation with  $T_d = 61.5$  degrees C is dominant and corresponds to melting of regions not bound to fatty acids. The second stage with  $T_d = 80$  degrees C corresponds to melting of regions bound to fatty acids. Serum denaturation heat is equal to 20.2 J/g dry protein.

The decomposition of peaks of the denaturation curve was made under the assumption that the denaturation of blood serum proteins occurs by the "all-or-none" principle. It is assumed that comparing the calculated melting parameters ( $T_d$ ,  $\Delta T_d$ ,  $\Delta H_d$ ,  $\Delta C_d$ ) of domains of blood serum proteins of donor with the corresponding parameters of patients with oncological and nononcological diseases can be used as a basis for a more precise diagnostics of these diseases.

### 1. Introduction

During some past years, the attention was more intensively focused on the physical methods that enable cancer diagnosis faster, at lower cost, and with higher preciseness. Namely, a

considerable attention is paid to diagnosis of new formations with lower antigen activities in comparison with hormonal embryonic formations.

### 2. Method and approach

The differential scanning microcalorimeter (SDC) enables us to study human blood, as well as human blood plasma and serum. It was demonstrated that the healthy human vein blood plasma and serum have a complex health absorption curve that repeats with allowed accuracy. It was determined that the heat absorption peaks and shoulders reflect denaturation of plasma/serum proteins. This fact gave us a possibility to use DSM as a new, cheap, and fast method of cancer diagnosis. The microcalorimetric analysis, as a cheap and quick





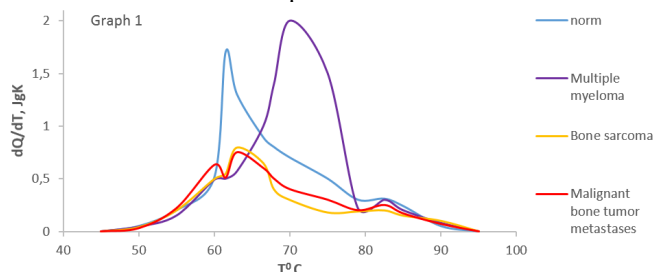
additional method has a potential to take its place among cancer diagnostic methods.

### 3. Results

Presented results are obtained after studying complex biological systems with differential scanning microcalorimeters (DSC) [1-6]. These studies have been performed on human whole blood [3], as well as on human blood plasma and/or serum [4-7]. It was demonstrated that the healthy human vein blood plasma and serum have a complex health absorption curve that repeats with allowed accuracy. It was determined that the heat absorption peaks and shoulders reflect denaturation of plasma/serum proteins. This fact gave us a possibility to use DSM as a new, cheap, and fast method of cancer diagnosis.

The experiments have revealed the following facts:

1. Independent melting of human blood plasma/serum main proteins
2. In solutions similar to human blood plasma/serum physiological conditions, content of main protein domains is almost the same as content of the domains in human blood plasma/serum
3. Healthy donor blood plasma/serum denaturation calorimetric curves are the same with reasonable preciseness
4. Healthy donor blood plasma/serum denaturation calorimetric curves differ from blood plasma/serum curves of non-cancer patients, and non-cancer blood plasma/serum denaturation calorimetric curves differ from cancer curves. Some microcalorimetric analysis curves of blood serum are demonstrated below in Graph 1.



Thanks to the fact that deconvolution of patient plasma/serum calorimetric curves clearly shows the heat absorption peaks that correspond melting of plasma/serum main proteins, we are able:

1. to compare  $\Delta H_d$ ,  $\Delta T_d$ ,  $\Delta T$ ,  $\Delta H_{max}$  denaturation parameters of healthy donor plasma/serum main proteins with the same parameters in case of a known disease and make a diagnosis that is expected to have 70% preciseness according to preliminary estimation;
2. to determine  $\Delta H_d$ ,  $\Delta T_d$ ,  $\Delta T$ ,  $\Delta H_{max}$  denaturation parameters of each domain in composition of each main protein by deconvolution of each peak of a main protein obtained after deconvolution of a calorimetric curve. Comparison of these parameters of healthy donors and patients with a known disease will give us a possibility to make a diagnosis at sub-molecular level – at level of small changes in small domains in composition of the main proteins. This will give us a unique possibility to increase preciseness of diagnosis to 90-95%.

This method has the following advantages:

1. The analysis requires little time

2. No chemicals are needed for the analysis
3. Not only quantity, but also quality changes of proteins are detected (i.e. structural changes of proteins such as point mutations, changes in chain length, redistribution of charge, lose of ligands, etc.).

From this viewpoint, albumin gives us some important information, because Ca, Fe, Cu, Zn, Mn ions, faticids, amino acids, hormones, different pharmaceutical agents and transferin bind to it. Also, Fe and Cu bind to ceruleoplasmins.

The advantage of microcalorimetry method is that DSM analysis enables us to detect a malignant process at molecular level.

Diagnostic possibilities:

1. Pre-surgery diagnosis of growing tumor
2. Assessment of treatment effectiveness
3. Pre-clinical detection of relapses and metastases
4. Post-surgery monitoring, detection of relapse, determination of remission.

The diagnosis consists of the following steps:

1. Deconvolution of blood plasma/serum to constituents that correspond to melting of the following proteins: albumin,  $\gamma$ -globulin, chemotrypsin,  $\alpha 2$ -microglobulin,  $\alpha 11$  globulins (ceruleoplasmin),  $\beta$ globulins (transferin, hemopexin)
2. Calculation of thermodynamic parameters ( $T$ ,  $\Delta T$ ,  $\Delta H$ ,  $\Delta C_{max}$ ) for each protein Calculation of  $H_{kal}/\square H_{Vg}$  ratio for each protein. This ratio indicates quantity of cooperatively melting structural domains.
3. The main product of the project – an experimental version of the calorimeter – is designed on the basis of the above studies and it meets all principal demands for diagnostics purposes.

### References

- [1] Madzhagaladze G.V., Monaselidze D.R., Chikvashvili R.I. Author's certificate of the USSR, N1267175, 1986 (in Russian).
- [2] Monaselidze J., Kalandadze I., Topuridze I., Gadabadze M., Khachidze D. "Diagnosis Method of Malignant Tumors", Priority 08.07.94, Patent of Georgia № Ge U 1994 985 U, Tbilisi (1994)
- [3] Monaselidze J., Kalandadze J., Topuridze I., Gadabadze M. High Temperatures High Pressures. 29 (1997), 677.
- [4] Gadabadze M., Khachidze D., Kalandadze Ya., Ghudushauri M., Monaselidze J., Topuridze I. "Differential Scanning Microcalorimeter as a Additional Method for Diagnosis of Bone Cancers". "Mkurnali" (Georgian). No 6-7. pp. 39-41, (1999)
- [5] Datikasvili D., Sresel R., Gadabadze M., Khachidze D., Topuridze I. Protein thermodynamic variations of blood serum from patients acute leukemia, Annals of Oncology, V. 16, p. 304, 2005.
- [6] Gadabadze M., Khachidze D. "Microcalorimetric parameters of blood plasma in Hodgkin's lymphoma". New in Hematology and Transfusiology, Kiev, Ukraine, pp.294-295 (2006, in Russian).
- [7] Monaselidze J., Kalandadze J., Topuridze I. 14th JUPAC, Conference on Chemical Thermodynamics, Osaka, Japan, 1996.
- [8] Khachidze D. and Monaselidze J. "Microcalorimetric study of human blood serum". Biophysics [IF SES 10(r)], vol. 45, №2, pp. 312-316, (2000).
- [9] Khachidze D. and Monaselidze J. "Independent denaturation of albumin and globulin in human blood serum". Biophysics, vol. 45, №2, pp. 317-319, (2000)
- [10] Putnam F.N., Marker Proteins in inflammation, New York, 1982. P1-12. Durdey P., Williams N.S., Brown D.A. Brit. J. Surg. 1984. V.71, p881-884.



# Validity of modified Maxwell-Garnett effective-medium Theory in Ferrofluids

L. Kalandadze<sup>1,a</sup>, O. Nakashidze<sup>1,b</sup>, N. Gomidze<sup>1,c</sup>, I. Jabnidze<sup>1,d</sup>

<sup>1</sup> Batumi Shota Rustaveli State University (BSU) Georgia

<sup>a</sup> [lali.kalandadze@bsu.edu.ge](mailto:lali.kalandadze@bsu.edu.ge), <sup>b</sup> [omar.nakashidze@bsu.edu.ge](mailto:omar.nakashidze@bsu.edu.ge), <sup>c</sup> [gomidze@bsu.edu.ge](mailto:gomidze@bsu.edu.ge), <sup>d</sup> [izolda.jabnidze@bsu.edu.ge](mailto:izolda.jabnidze@bsu.edu.ge)

**Abstract.** Investigation of the optical properties of ferrofluids is an important task aimed at the study of structural characteristics of ultrafine structures. The optical spectra of ultrafine structures strongly depend on composition and dielectric constants of particles and matrix. In its turn, the dielectric constants are functions of the structural and electronic parameters and can differ from those for corresponding bulk materials. This article reports on the results obtained in the experimental and theoretical studies of the diagonal components of the tensor of dielectric permittivity of the ferrofluids. For experimental investigation of the diagonal components of the tensor of dielectric permittivity, we have selected the Avery method. The effective diagonal components of the tensor of dielectric permittivity of the nanostructures are represented within the modified effective medium approximation theory. In this approach, optical characteristics can be calculated as a function of the matrix, volume fraction of the ferromagnetic particles and particle shape. This theory gives a good opportunity to forecast the optical properties of the ultrafine medium and therefore, to receive the proper parameters of ultrafine medium,

## 1. Introduction

It is known that the qualities of already explored materials change in the process of their transformation into nanocrystals [1, 2]. This was predictable because these structures contain from some atoms to thousands of atoms and take a middle place between atoms and massive substances, and subsequently, they have properties different from both of them. Nowadays, cutting-edge technology makes it feasible to devise materials with new structures and new properties, which would widen the boundaries of their use. There is no doubt that the experimental and theoretical data about this topic stimulates the enormous interest, because there is the paucity of knowledge and the need to explain a lot in the area of physics concerning nanostructures and the modern materials.

Depending on the size of the nanostructure, the interaction of light with structured materials can be very different. The optical spectra of nanostructures strongly depend on composition and dielectric constants of particles and matrix. The dielectric constants are functions of the structural and electronic parameters and can differ from those for corresponding bulk materials [3-6]. Thus, optical spectra investigations can give very useful information about structural parameters of the ultrafine structures. Ultrafine medium is an ensemble of particles having smaller size than 100 nm.

In this paper we consider the theoretical Maxwell-Garnett model that have been devised for relating optical properties of composite materials to those of the constituent materials and to the morphology of the composite structure. We also survey experimental studies aimed at validating this model.

For this purpose, we present theoretically and experimentally the influence of the structural parameters on the optical properties of thin iron films and Fe<sub>3</sub>O<sub>4</sub> nanoparticles. In this respect, it is possible to look at how

theoretical model describes the optical properties of magnetic nanostructures according to the experimental data.

## 2. Theory

Optical properties of ultrafine structures discovered the interpretation in the effective-medium approximation models, which in the optical case define effective dielectric function from averaged fields. Till now, the Maxwell-Garnett theory is the most popular in the description of optical properties of nanostructures [7-11].

It is known that the Maxwell-Garnett theory has been educated for optically isotropic medium with scalar dielectric constants [9]. The theory concerns a ultrafine structures, consisting of random particles of more than two varieties of substances, as a homogeneous effective medium which has an effective dielectric tensor in a given wavelength region. That means, that the sizes of these heterogeneities, are much less than the light wavelength. Therefore, we cannot differ each compound coupled in the effective medium. In the Maxwell-Garnett theory ultrafine structure or composites could be substituted by an appropriate effective medium with an effective dielectric constant.

We have modified the Maxwell-Garnett model to investigate nano-dispersive medium with optically anisotropic particles (ellipsoids). After generalization of the Maxwell-Garnett theory for ultrafine structure which composed of ellipsoidal particles or inclusions with different dielectric permittivity  $\epsilon_i$  ( $i = 1, 2, 3, \dots, n$ ) and matrix (host medium) with dielectric permittivity  $\epsilon_m$  we arrived at formula how to calculate diagonal elements of the dielectric tensor for non-spherical ultrafine particles.

$$\frac{\epsilon_{ef} - \epsilon_m}{\epsilon_m + f(\epsilon_{ef} - \epsilon_m)} = \sum_i^n q_i \cdot \frac{\epsilon_i - \epsilon_m}{\epsilon_m + f(\epsilon_i - \epsilon_m)} \quad (1)$$

Where  $\epsilon_{ef}$  is effective dielectric permittivity of nano-dispersive structure,  $q$  is the ratio of the volume with particles to the total volume of the ultrafine medium and  $f$  is the shape factor of the nanoparticles.

Equation (1) has been obtained in the following assumptions. First, the structure is composed of identical ellipsoids that similarly oriented in an external electric field  $\vec{E}_0$ . Second, the polarizability  $\alpha_i$  of the nanoparticles with dielectric permittivity  $\epsilon_i$  is given by [10]

$$\alpha_i = \frac{V_i}{4\pi} \frac{\epsilon_i - \epsilon_m}{\epsilon_m + f(\epsilon_i - \epsilon_m)} \quad (2)$$

The effective dielectric permittivity  $\epsilon_{ef} = \epsilon_{1ef} - \epsilon_{2ef}$  is linked to reflective index  $n_{ef}$  and absorption index  $k_{ef}$  of nano-dispersive medium by formula:



$$\varepsilon_{ef} = (n_{ef} + ik_{ef})^2. \quad (3)$$

If a nano-dispersive medium has ellipsoidal particles with dielectric permittivity  $\varepsilon_i = \varepsilon$ , eq. (1) can be expressed as:

$$\frac{\varepsilon_{ef} - \varepsilon_m}{\varepsilon_m + f(\varepsilon_{ef} - \varepsilon_m)} = q \frac{\varepsilon - \varepsilon_m}{\varepsilon_m + f(\varepsilon - \varepsilon_m)}. \quad (4)$$

For spherical particles  $f=1/3$ , using eq. (2), we can obtain the Maxwell-Garnett formula [12]:

$$\frac{\varepsilon_{ef} - \varepsilon_m}{\varepsilon_{ef} + 2\varepsilon_m} = q \frac{\varepsilon - \varepsilon_m}{\varepsilon + 2\varepsilon_m}. \quad (5)$$

We assumed that formula (2) would be valid for  $q \geq 0.5$ . If  $q \geq 0.5$  Structure can be represented as a metal (matrix) with the volume fraction of dielectric inclusions  $q$ . In this case eq. (2) can be written as:

$$\frac{\varepsilon_{ef} - \varepsilon}{\varepsilon + f'(\varepsilon_{ef} - \varepsilon_m)} = (1-q) \frac{\varepsilon_m - \varepsilon}{\varepsilon + f'(\varepsilon_m - \varepsilon)}, \quad (6)$$

where  $q$ ,  $\varepsilon$  and  $\varepsilon_m$  are replaced by  $(1-q)$ ,  $\varepsilon_m$  and  $\varepsilon$  respectively;  $f'$  is the shape factor of the dielectric inclusions.

### 3. Experimental details

The ferrofluids were prepared on the base of  $Fe_3O_4$  and Fe particles with average size approximately 5 nm in different carrier fluids (water, kerosene, silicon-organic compound).

The most widely used optical methods are the ellipsometry and the methods which study the intensity of the light reflected from the sample (method Avery). In this work for determining the optical properties we have chosen the Avery method [13].

### 3. Results

The exploration of the spectral dependences of the diagonal components  $\varepsilon_1$  and  $\varepsilon_2$  of the tensor of dielectric permittivity has shown that for nano-dispersive structures based on particles of magnetic oxides the character of spectral dependences of diagonal components of the tensor of dielectric permittivity is similar for the magnetic particles and the substance of particles. Whereas for nano metal films the character of the spectral dependences of the diagonal components  $\varepsilon_1$  and  $\varepsilon_2$  of the tensor of dielectric permittivity is significantly different from that of the similar spectral dependences for polycrystalline metal and depends on the effective weight thickness of the films. [ 4-6 ].

Fig. 1 gives experimental and theoretical dependences of the diagonal components  $\varepsilon_1$  (a) and  $\varepsilon_2$  (b) of the tensor of dielectric permittivity on the quantum energy of incident light  $\hbar\omega$  for the magnetite magnetic particles in kerosene, for its sediments and for a bulk film  $Fe_3O_4$ . For the theoretical calculations we have used modified Maxwell-Garnett model (eq. (4)) to interpret experimental spectra of the diagonal components of the tensor of dielectric permittivity for ultrafine structures.

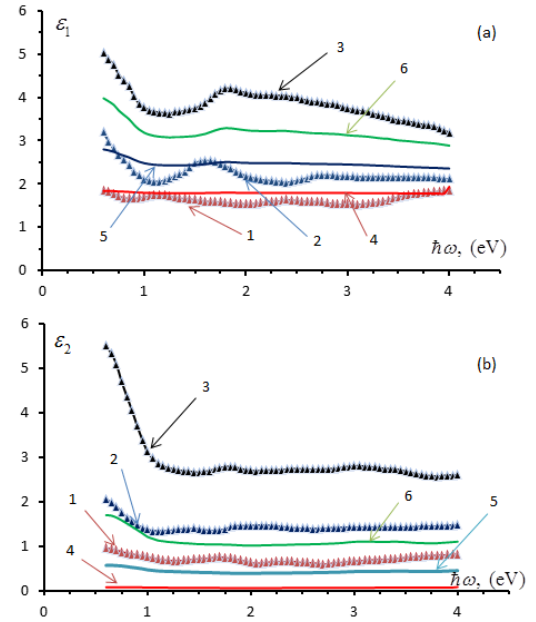
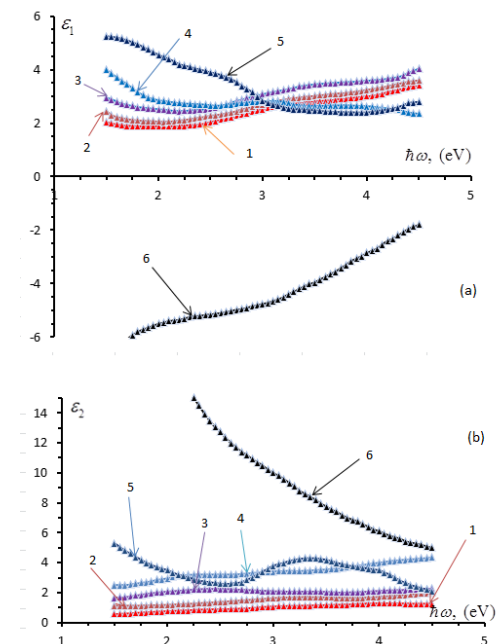


Fig.1. Experimental dependences of the diagonal components  $\varepsilon_1$  (a) and  $\varepsilon_2$  (b) of the tensor of dielectric permittivity on the quantum energy of incident light  $\hbar\omega$  for magnetite magnetic fluids (1), for its sediments (2) and for bulk film  $Fe_3O_4$ . Theoretical dependences of  $\varepsilon_{1ef}$  and  $\varepsilon_{2ef}$  for magnetite particles with  $q=0.05$  (curve 4);  $0.25$  (curve 5);  $0.5$  (curve 6);  $\varepsilon_m=2.25$ ;  $f=1/3$

Comparing the experimental data with the theoretical results for magnetite particles we observe that (Fig. 1(a) and (b)) the spectra of the diagonal components  $\varepsilon_1$  and  $\varepsilon_2$  of the tensor of dielectric permittivity are similar to the spectral dependences calculated with different  $q$ .

Fig. 2 gives experimental dependences of the diagonal components  $\varepsilon_1$  (a) and  $\varepsilon_2$  (b) of the tensor of dielectric permittivity on the quantum energy of incident light  $\hbar\omega$  for nano-dispersive iron films with different weight thicknesses and polycrystalline Fe.





**Fig.2.** Experimental dependences of the diagonal components  $\varepsilon_1$  (a) and  $\varepsilon_2$  (b) of the tensor of dielectric permittivity on the quantum energy of incident light  $\hbar\omega$  for thin iron films with weight thicknesses  $d=8.8$  nm (curve 1); 13.0 nm (curve 2); 5.4 nm (curve 3); 12.0 nm (curve 4); 11.2 nm (curve 5) and polycrystalline Fe (curve 6).

It follows from the Fig. 2 that the character of frequency dependences of the diagonal components  $\varepsilon_1$  (a) and  $\varepsilon_2$  (b) of the tensor of dielectric permittivity for the thin iron films depends on the weight thickness of the films and is meaningfully different from the similar spectral dependences for polycrystalline iron.

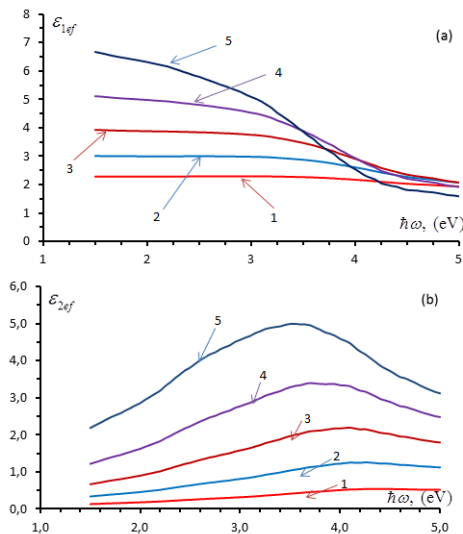


**Fig.3.** Dependences of the diagonal components  $\varepsilon_{1ef}$  (a) and  $\varepsilon_{2ef}$  (b) of the tensor of dielectric permittivity on the quantum energy of incident light  $\hbar\omega$  for nano-dispersive Fe films calculated by formulas (4) with  $q=0.1$  (curve 1), 0.2 (curve 2), 0.3 (curve 3), 0.4 (curve 4), 0.5 (curve 5) and  $f=1/3$ ;  $\varepsilon_m=1.69$

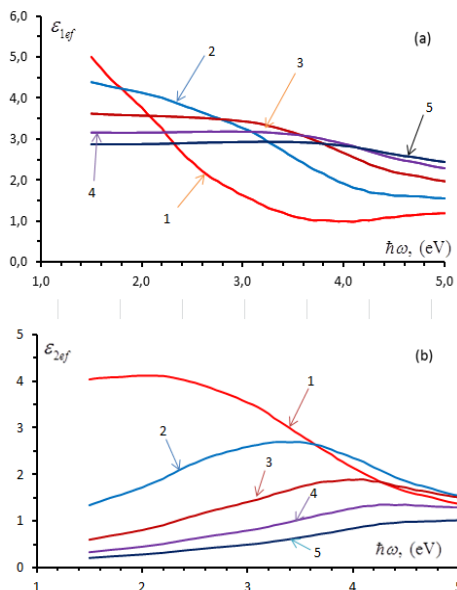


**Fig.4.** Dependences of the diagonal components  $\varepsilon_{1ef}$  (a) and  $\varepsilon_{2ef}$  (b) of the tensor of dielectric permittivity on the quantum energy of incident light  $\hbar\omega$  for nano-dispersive Fe films calculated by formulas (4) with  $f$

$=0.1$  (curve 1), 0.2 (curve 2), 0.3 (curve 3), 0.4 (curve 4), 0.5 (curve 5) and  $q=0.25$ ;  $\varepsilon_m=1.69$

Fig. 3 gives theoretical dependences of the diagonal components  $\varepsilon_{1ef}$  (a) and  $\varepsilon_{2ef}$  (b) of the tensor of dielectric permittivity on the quantum energy of incident light for thin iron films with various  $q$ . In this case spectrum character of the  $\varepsilon_{1ef}$  and  $\varepsilon_{2ef}$  is practically the same.

We have also calculated the dependences of the diagonal components of the tensor of dielectric permittivity on the quantum energy of incident light for nano-dispersive Fe with different  $f$ .

It could be seen from the Fig.4 (a, b) that for the Fe films the spectral dependences of the diagonal components of the tensor of dielectric permittivity depend on the shape factor of the nanoparticles.

Analysis of the experimental and theoretical results obtained gives that for nano-dispersive structures based on particles of magnetic oxides, for the optical constants of the material of which  $k^2 \ll n^2$  holds the character of spectral dependences of  $\varepsilon_1$  and  $\varepsilon_2$ , is similar for the magnetic particles and the substance of particles. Whereas for the nano-dispersive Fe films with a various thickness  $d$  the character of the spectral dependences of the diagonal components is meaningfully different from that of the similar spectral dependences for polycrystalline Fe ( $k \approx n$ ) and depends on the effective weight thickness of the films. Modified the Maxwell-Garnett effective-medium theoretical model shows that if we take into account the shape factor of the particles, we will achieve agreement of the experimental results and the theoretical calculations.

### Conclusions

To verify the suitability of the modified Maxwell-Garnett effective-medium theoretical model we have considered theoretically and experimentally the impact of the structural parameters on the diagonal components of the tensor of dielectric permittivity of the Fe<sub>3</sub>O<sub>4</sub> particles and discontinuous Fe films. The behavior of the frequency dependences of the diagonal components of the tensor of dielectric permittivity for the magnetite particles in various media and thin Fe films was elucidated in the framework of model of the effective medium approximation. In this approach effective diagonal components of the tensor of dielectric permittivity of the ultrafine structures can be calculated as a function of the ratio of the volume with particles to the total volume of the ultrafine medium and particle shape factor. Furthermore, the experimentally derived data are compatible with the above considered theory.

### References

- [1] Benozir A., Narain R. Chapter 15 - Nanomaterials properties, Polymer Science and Nanotechnology, (2020) 343-359. <https://doi.org/10.1016/B978-0-12-816806-6.00015-7>
- [2] Machon D., Pishedda V., Le Floch S., San-Miguel A. Perspective: High pressure transformations in nanomaterials and opportunities in material design, J. of Applied Physics 124, (2018) 160902. <https://doi.org/10.1063/1.5045563>
- [3] Kalandadze L., Nakashidze O. Influence of the Size, Shape and Concentration of Magnetic Particles on the Optical Properties of Nano-



- dispersive Structures, *J. Magnetism and Magnetic Materials*, 500, (2020) 166355. <https://doi.org/10.1016/j.jmmm.2019.166355>
- [4] Kalandadze L., Nakashidze O., Gomidze N., Jabnidze I. Theoretical and Experimental Investigation of the Optical Properties of Nano Nickel Films, *IEEE 8th International Conference on Advanced Optoelectronics and Lasers (CAOL)*, (2019), 1-4 DOI: [10.1109/CAOL46282.2019.9019538](https://doi.org/10.1109/CAOL46282.2019.9019538)
- [5] Gehr R. J., Bovd R.W. Optical Properties of Nanostructured Optical Materials, *Chem. Mater.* 8, 8, (1996) 1807-181, <https://pubs.acs.org/doi/10.1021/cm9600788>
- [6] Kelly K.L., Koronado E., Shao L.L., Schatz G.C. The Optical Properties of Metal Nanoparticles, *J. Phys. Chem. B*, 107,3 (2003) 668-677. <https://doi.org/10.1021/jp026731v>
- [7] Nikitin L.V., Kalandadze L.G., Akhmedov M.Z., Nepijko S.A. Journal Magnetism and Magnetic Materials 148 279, (1995) DOI: [10.1016/0304-8853\(95\)00236-7](https://doi.org/10.1016/0304-8853(95)00236-7)
- [8] Levy O., Stroud D. Maxwell Garnett theory for mixtures of anisotropic inclusions: Application to conducting polymers, *Phys. Rev. B* 56, (1997), 8035. DOI: <https://doi.org/10.1103/PhysRevB.56.8035>
- [9] Nakashidze O., Kalandadze L. Influence of Shape of Magnetic Particles on the Magneto-Optical and optical Properties of the nano-dispersive cobalt 2016 IEEE 7<sup>th</sup> International Conference on Advanced Optoelectronics and Lasers; (2016), 17-20. DOI: [10.1109/CAOL.2016.7851360](https://doi.org/10.1109/CAOL.2016.7851360)
- [10] Markel V.A. Introduction to the Maxwell Garnett approximation, *Journal of the Optical Society of America A*, 33, 7 (2016) 1244-1256 <https://doi.org/10.1364/JOSAA.33.001244>
- [11] Wormeester H., Kooij E., Poelsuma B. Effective dielectric response of nanostructured layers. *Phys Stat Sol (a)* (2008) 205:756-763. <https://doi.org/10.1002/pssa.200777740>
- [12] J.C. Maxwell Garnett. XII. Colours in metal glasses and in metallic films, *Philosophical Transactions of the Royal Society of London. Series A, Containing Papers of a Mathematical or Physical Character*, 203:385-420. <https://doi.org/10.1098/rsta.1904.0024>
- [13] Avery D. An improved method for measurement of optic constants by reflection, *Proc. Phys. Soc. London (B)*, 65 (1952) 426 – 429. DOI: [10.1088/0370-1301/65/6/305](https://doi.org/10.1088/0370-1301/65/6/305)

## 3D fluorescence spectroscopy to study the distribution of bioparticles

N. Gomidze<sup>1,a</sup>, J. Shainidze<sup>1,b</sup>, M. Khajishvili<sup>1,c</sup>, I. Jabnidze<sup>1,d</sup>, K. Makharadze<sup>1,e</sup>,  
L. Kalandadze<sup>1,f</sup>, O. Nakashidze<sup>1,g</sup>, Z. Surmanidze<sup>1,h</sup>, E. Mskhaladze<sup>2,i</sup>, L. Gomidze<sup>3,j</sup>

<sup>1</sup> Batumi Shota Rustaveli State University, Batumi, Georgia

<sup>2</sup> Batumi Maritime Academy, Batumi, Georgia

<sup>3</sup> Tbilisi State University, Tbilisi, Georgia

<sup>a</sup>[gomidze@bsu.edu.ge](mailto:gomidze@bsu.edu.ge) <sup>b</sup>[jabashainidze@gmail.com](mailto:jabashainidze@gmail.com), <sup>c</sup>[miranda.khajishvili@bsu.edu.ge](mailto:miranda.khajishvili@bsu.edu.ge), <sup>d</sup>[izolda.jabnidze@bsu.edu.ge](mailto:izolda.jabnidze@bsu.edu.ge),

<sup>e</sup>[k.makharadze.01@gmail.com](mailto:k.makharadze.01@gmail.com), <sup>f</sup>[lali.kalandadze@bsu.edu.ge](mailto:lali.kalandadze@bsu.edu.ge), <sup>g</sup>[omar.nakashidze@bsu.edu.ge](mailto:omar.nakashidze@bsu.edu.ge),

<sup>h</sup>[zebur.surmanidze@bsu.edu.ge](mailto:zebur.surmanidze@bsu.edu.ge), <sup>i</sup>[eldar@bsma.edu.ge](mailto:eldar@bsma.edu.ge), <sup>j</sup>[lukagomidze@gmail.com](mailto:lukagomidze@gmail.com)

**Abstract.** Common methods of analysing the chemical composition of a substance include many existing optical methods. Selecting an effective and optimal method from numerous optical methods and adapting it to the properties of the investigated substance is one of the most urgent tasks of modernity. Scientists are trying to study the substances – bio-nano-agents that surround humanity and develop methods and approaches that are used in one way or another to study materials. The properties of materials are determined by considering both, the main components and the compounds. In addition, often the properties of the materials depend on the distribution of the compounds or components in its volume. Modern fluorescent spectrometers are economical, portable devices and they are easy to use in the outside conditions for investigation of biological structure, environment and clinical studies. But to obtain high-throughput spectra expensive stationary equipment is still needed. In addition, its operation requires properly trained staff. Nevertheless, it is possible to use portable spectrometers equipped with fiber-optic wires for high scientific purposes. So, for example the company StellarNet's portable spectrometer Black Comet and light source NL-100 (nitrogen laser, 0-25 Hz), also, computation of optical and electronic components with open software interface SpectraWiz allows us to obtain high quality 3D fluorescence spectra. Open code spectrometer can give new opportunities in research and education.

### 1. Introduction

Today, the growing interest in laser fluorescence spectroscopy is due to its practical application in laser communication, ecology, and medicine. Medical imaging, for example, is one of the major problems in medicine.

A number of works have already been performed to increase the characteristics of the detected signal. For example,

spectra of emission radiation intensity of blood plasma were measured [1], where a partially coherent laser beam fell on the blood plasma placed in the cuvette and the intensity of the scattered laser radiation was also intensified.

In another work [2] was discussed the relationship of stochastic shifts in solutions and gases to the wavelength of the absorbed light. Scattering from water molecules (Raman scattering) has been studied in the paper [3]. Fluorescence characteristics such as fluorescence attenuation and damping dependence on wavelength, quantum yield, and fluorescence damping time are studied in the paper [4]. Fluorescence anisotropy and fluorescent energy transfer conditions have been studied in the paper [5].

In the paper [6] it has been shown that partial spatial coherence of the source reduces scintillation. The partial coherence function of a partially coherent Gaussian source is studied in paper [7]. The properties of the Gaussian beam, such as average intensity, beam width, phase front radius of curvature, wave front coherence radius was investigated in [8]. Analysis of radius of the partially spatial coherence beam is presented in [9].

Under conditions of weak and strong turbulence, an analytical image of the partially spatial coherence beam intensity correlation function was obtained in the paper [10,11]. [12] paper investigates the scintillation effect for a



partially temporal coherence wave.

Within grant project №FR-152-9-240-14 [13-15] was taken spectra using spectrometer StellarNet Black-Comet (190-900 nm) which captures of laser beams scattered from an optically dense random phase screen.

The difficulty is otherwise - to evaluate the statistical characteristics of the signal detected through a heterogeneous environment and to visualize the spectral image. These difficulties are caused by environmental statistics. For example, the detection of fluorescence signals in complex environments and the visualization of spectral images are associated with significant difficulties, because the complex composition of the environment (petroleum, petroleum products, organic compounds, etc.) determines the overlap of spectra and reduces the ability to decipher useful information. It becomes important to increase the quality of the signal registered on the detector and to determine the factors that are responsible for this quality.

## 2. Theoretical part

The quantum theory of radiation pictures atoms with quantized energy levels interacting with an assembly of photons of varying frequencies  $\omega$ . When the energy difference between two atomic states fulfills a resonance condition  $\hbar\omega = E_1 - E_0$ , three possible transition processes can occur: absorption, stimulated emission, and spontaneous emission. In the electric-dipole approximation, the transition rates for absorption and stimulated emission are given by [21]:

$$W_{abs} = W_{stim\ em} = \frac{4\pi^2}{3\hbar^2} \rho(\omega) |\langle 0|\mu|1\rangle|^2,$$

where  $\mu$  is the electric dipole operator and  $\rho(\omega)$  is the spectral density of the radiation field at frequency  $\omega$ . The corresponding rate of spontaneous emission is:

$$W_{spont\ em} = \frac{4\omega^2}{3\hbar c^3} |\langle 0|\mu|1\rangle|^2.$$

All three radiative processes depend on the matrix element  $\langle 0|\mu|1\rangle$  and therefore obey the same selection rules. A convenient measure of the intensity of a transition is the oscillator strength:

$$f_{0,1} = \frac{2m_e\omega}{3\hbar e} |\langle 0|\mu|1\rangle|^2,$$

which generally lies in the range from 0 to 1. The dependence on  $\omega^3$  makes spontaneous emission significant only for higher-energy transitions—in practice, only for optical frequencies and higher. The Figure 1 shows considers the transition-energy range of 0.1 to 10 eV, corresponding to radiation wavelengths of 12000 to 120 nm, which includes the visible region 380–750 nm, as well as parts of the infrared and ultraviolet.

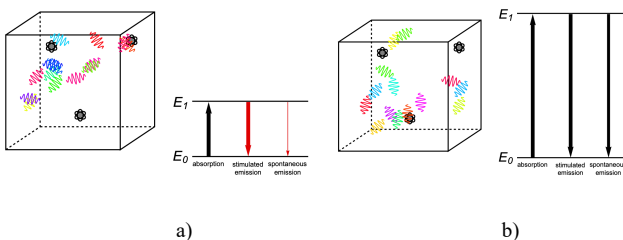


Fig.1. Demonstration of transition processes: a) transition in the infrared region  $E_1 - E_0 = 0, 2$  eV,  $\lambda = 6200$  nm,  $f_{0,1} = 0, 5$ ; b) transition in the ultraviolet region  $E_1 - E_0 = 10$  eV,  $\lambda = 120$  nm,  $f_{0,1} = 0, 5$

The electromagnetic field is governed by the same equations as the quantum harmonic oscillator. The probabilities for annihilation and creation of a photon of frequency  $\omega$  are given by:

$$|\langle n_\omega - 1 | a_\omega | n_\omega \rangle|^2 = n_\omega,$$

and

$$|\langle n_\omega + 1 | a_\omega^+ | n_\omega \rangle|^2 = n_\omega + 1,$$

respectively. The photon numbers  $n_\omega$  are proportional to the spectral density  $\rho(\omega)$ , while the additional term +1 in the creation formula accounts for the phenomenon of spontaneous emission.

When tissue is penetrated, the dominant effects are scattering and absorption by polarizable bio-particles. The most important parameter in the interaction is the power density,  $s(r, z)$  ( $mW/mm^2$ ). This is a function of power source delivered from an optical radiation source to the biological tissue, where input power is  $P(W)$ , and the spot has a radius  $R(mm)$ . The propagation of the scattered radiation is described by the photon transport equation [22]:

$$(s\nabla)L(r, s) = \frac{dL}{ds} = -\mu_s L(s, s') + \mu_s \int_{4\pi} P(s, s') L(s, s') ds.$$

We can expand the plane waves in terms of Legendre polynomials to find an expression from the scattering amplitude and the differential cross section:

$$f(\theta, \varphi) = \frac{1}{4\pi} \int e^{i(\vec{k}\vec{r})} U(\vec{r}) d\vec{r},$$

$$\frac{d\sigma}{d\Omega} = \frac{1}{k^2} \left| \sum_{l=0}^{\infty} (2l+1) e^{i\delta} \sin\delta P_l(\cos\theta) \right|^2,$$

where  $U(\vec{r})$  is the potential energy. The amplitude  $f(\theta, \varphi)$  depends on the potential, the scattering angle  $\theta$ , and the target area  $\varphi$ . The total cross section is:

$$\sigma_T = \frac{4\pi}{k^2} \left| \sum_{l=0}^{\infty} (2l+1) e^{i\delta} \sin^2\delta \right|^2,$$

We verify directly that:

$$\sigma_T = \frac{4\pi}{k^2} \text{Im} f(0).$$

which is called the optical theorem. So, we can find power factor on optical radiation penetration in tissue depth and analyze depends power factor on wavelength for different scattering and absorption factor:

$$s(\lambda, P, \delta, d) = \frac{55P}{4\pi\delta^2 \cdot 0.01} \exp \left[ -0.1 \left( \frac{\sin(0.5)}{\lambda} \right)^2 + \frac{d}{\delta} \right].$$

Fig. 2 show that changing the wavelength from shorter to longer slightly increases the power factor in the volume of bioparticles (measured in  $mW/mm^2$ ). This means that shorter wavelengths generate heat more than longer wavelengths. Longer wavelengths remain constant with changes in tissue depth due to the penetration of photon radiation  $d$ , as well as due to the properties of the optical thickness of the tissue  $\delta$ . Other factors include a change in the source of the radiation power  $P$  and a change in the wavelength  $\lambda$ , as well as the angle of incidence of the radiation photons  $\theta$ . Since heat generation is caused by the radiation beam propagation through highly



water-absorbing tissue, the intensity is exponentially attenuated due to the low scattering factor.

This model includes several assumptions: 1) Scattering process is elastic, which means that the frequencies of incident and scattered radiation are the same. 2) Any interaction between the scattering bio-particles is neglected, therefore, we don't take into account the process of multiple scattering. 3) The width of the incident beam is much larger than the width of the scattered beam, hence the bioparticle will have a well-defined momentum.

When a diatomic molecule undergoes a transition to an excited electronic state higher by  $\Delta E_{elec}$ , it generally changes its vibrational and rotational quantum numbers as well. In the liquid state, the individual rotational levels are not generally resolved and the resulting process is characterized as a *vibronic transition*. Both the ground and excited electronic states are represented by potential energy curves, shown in blue and red, respectively, on the figures 3. The probability densities of the first few ground state and excited-state vibrational levels,  $|U_{v_1}^{(0)}|^2$  and  $|U_{v_2}^{(1)}|^2$ , are shown, superposed on the vibrational energy-level diagrams, with  $v = 0, 1, 2 \dots$ . Here the superscripts refer to the electronic state, while the subscripts label the vibrational level.

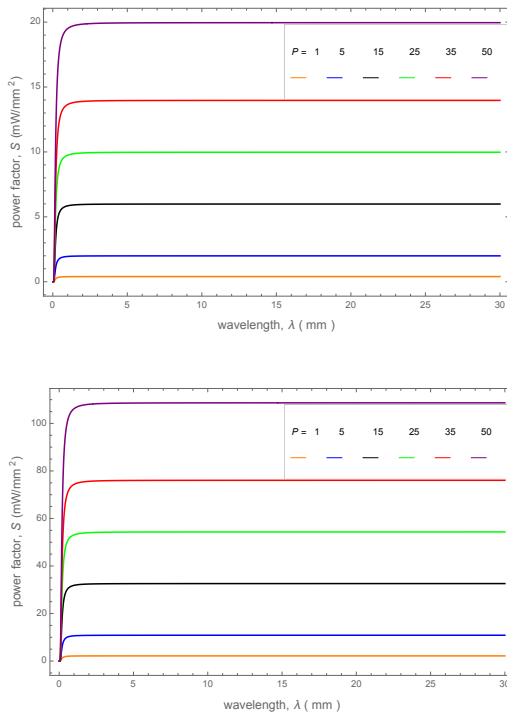


Fig 2. Power factor on optical radiation penetration in optical and tissue depth for analysis of scattering and absorption factor a)  $d = 7 \text{ mm}$ ,  $\delta = 1 \text{ mm}$ , b)  $d = 7 \text{ mm}$ ,  $\delta = 10 \text{ mm}$

At normal temperatures, only the  $v = 0$  vibrational level of the ground state is occupied. When a molecule absorbs a photon in an electronic transition, the electrons can rearrange themselves much more rapidly than the much heavier nuclei (consistent with the Born–Oppenheimer approximation). Thus, electronic transition can be approximated by the vertical blue arrow to internuclear distances  $R$  in the excited state very close to its maximum value in the ground state. This leads to a mixture of several excited-state vibrational levels,

predominated by the level that completely overlaps with the  $U_0^{(0)}$  wavefunction. According to the Franck–Condon principle, the relative intensities of the individual vibrational peaks are proportional to the factors  $|\langle U_{v_2}^{(1)} U_0^{(0)} \rangle|^2$ . This gives rise to an absorption spectrum shown in blue. The relative intensity of the vibrational components depends on the molecular parameters of the two electronic states, but most sensitively on the difference between equilibrium internuclear distances,  $R_0$  and  $R_1$ .

A molecule excited in an electronically allowed transition will generally return to its ground electronic state, a process called *fluorescence*, within the order of a few nanoseconds. Before it does so, most of the excited molecules will decay to the lowest vibrational state  $U_0^{(1)}$  by radiationless transition processes, such as internal collisional processes between molecules. These are represented in the upper curve by a series of black arrows. Fluorescence will then produce a series of peaks corresponding to different vibrational levels of the ground state, with intensities proportional to the Franck–Condon factors  $|\langle U_{v_1}^{(0)} U_0^{(1)} \rangle|^2$ . Because of the geometry of the energy curves, the fluorescent spectrum is very nearly a mirror image of the absorption spectrum, with the transitions  $v_1 = 0 \leftrightarrow v_2 = 0$ , meaning that this same transition occurs in both the absorption and fluorescence spectra. Figure 3 shows the Franck–Condon factors and spectral intensities are simulated since explicit computation would take too long [23].

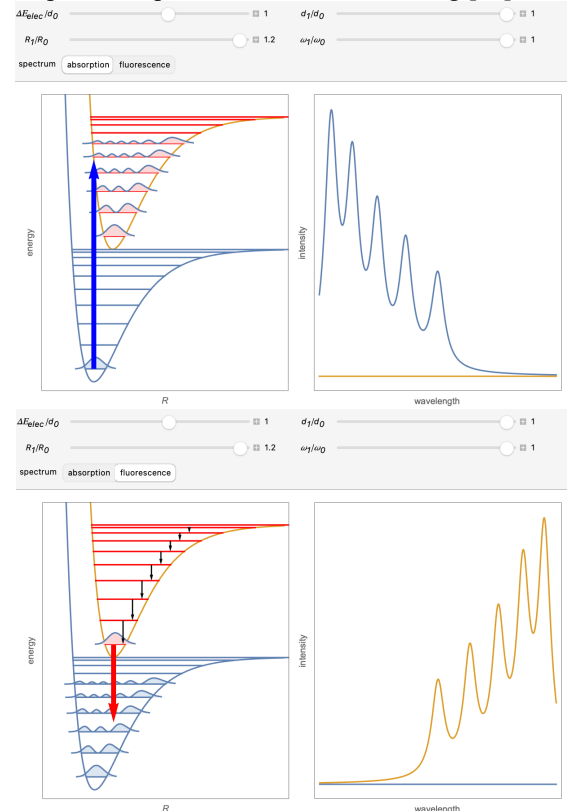


Fig. 3.  $\frac{\Delta E_{elec}}{d_0} = 1$ ,  $\frac{R_1}{R_0} = 1.2$ ,  $\frac{d_1}{d_0} = 1$ ,  $\frac{\omega_1}{\omega_0} = 1$  a) the vibrational peaks in the absorption spectrum are notated, right to left. The peak is dominant here since  $R_0$ , and  $R_1$  differ only slightly. b) corresponding fluorescence spectrum; the peaks are notated, left to right

## 2. Methodology, discussion and applications



Suppose  $(x_1, z_1)$  the coordinates of a beam of light for an optical system are known. After passing through the phase screen, the coordinates of the beam are transformed by the matrix equation:

$$\begin{bmatrix} z_2 \\ x_2 \end{bmatrix} = \begin{bmatrix} A & B \\ C & D \end{bmatrix} \begin{bmatrix} z_1 \\ x_1 \end{bmatrix}$$

where  $x_1 = \varepsilon \theta$ ,  $\varepsilon$  - is the refractive index of the media at the point where the beam falls,  $\theta$  is the angle between the direction of propagation of the beam and the optical axis. The determinant of the beam transmission matrix is the ratio of the refractive index to the input and output of the optical system. Such an approach allows us to study dependence of scintillation index  $\sigma$  a random phase screen on the correlation radius of the diffuser and the distance from the diffuser. Capturing and then visualizing the detected signal spectrum is one of the most important tasks in medical physics. The realization of visualization is carried out using appropriate mathematical methods. The object of study can be considered as a linear system that determines the transformation of the primary signal. Important part is the computation of the matrix of this transformation by mathematical methods. In principle, formation of the visual image involves receiving a medical signal, forming it using reconstruction techniques, then analyzing and evaluating the medical image (Fig.4).

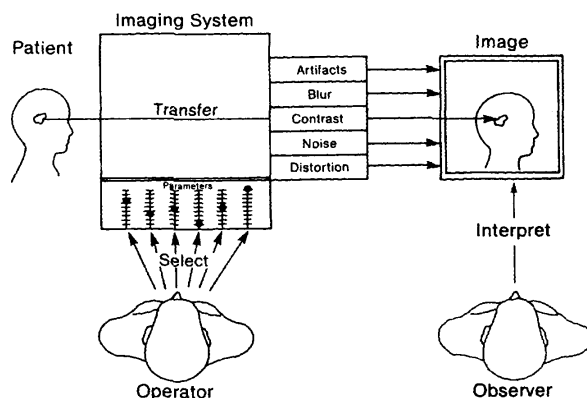


Fig. 4. General scheme of medical image visualization

As can be seen from the diagram, five components are important: the patient, the image formation system, the operator system, the image, and the observer. According to the task, we currently have different systems, such as: X-ray radiology, radioisotope radiation formation systems, magnetic resonance, ultrasound systems. In each method it is possible to control different physical parameters by the operator, for example: change of potential in the X-ray tube, controls of the concentration and type of radioisotopes, control of the magnetic field gradient and characteristic times, etc.

There are different methods for creating or registering a medical image. For example: photographic plate coverage, gamma camera, digital detectors and others. In the end, the image is analyzed by the observer to obtain structural (anatomical) or in some cases functional (physiological) information. Of course, it is up to the observer to detect a number of pathologies, however the latter depends on three factors at the same time: the quality of the image, the condition of the observation, the physical characteristics of the observation. The image itself depends on 5 factors: contrast,

resolution (spatial resolution), background noise, artifacts and distortions. It is these factors that contribute to the high quality of the image in the process of its formation.

Different radiations have different scales of resolution, for example: the range of vision for gamma radiation is in the range of 10-3 mm, 5-2 mm for ultrasound, 3-1 mm for magnetic resonance, 2-0.8 mm for tomography, fluoroscopy 1-0.4 mm, conventional radiography 0.5-0.1 mm, mammography below 0.05 mm.

Suppose experimental measurements are carried out on the object under examination by the selected method. Assume that some physical characteristic parameters were taken into account when performing  $N$  independent measurements:

$$x_1, x_2, x_3, \dots, x_i, \dots, x_N,$$

to each  $x_i$  measured value Corresponds only integer number. The main characteristics of these data are their sum and average size:

$$\Sigma \equiv \sum_{i=1}^N x_i, \quad \bar{x}_e \equiv \frac{\Sigma}{N}.$$

The distribution of sets  $x_i$  can be represented by the distribution function  $F(x)$ , which is the relative frequency at which  $x$  takes values from the database described above. Frequency allocation is automatically normalized to 1:

$$\sum_{x=0}^{\infty} F(x) = 1.$$

Let us considered that process of detection is binary. We can have only two outcomes: "success" or "failure". The probability of success can be conditionally denoted by  $P$ , which we consider to be constant for all experimental trials. The number of experiments can usually be denoted by  $N$ .

Under certain conditions we might predict a distribution function that describes a process. Let us distinguish three well-known statistical models: 1. Binomial distribution - one of the most general and usable in computational calculations; 2. Poisson distribution - a relatively simplified model when  $P$  is small and  $N$  is large; 3. Gaussian or Normal Distribution - an even more simplified model when the average probability of success is relatively high.

By binomial distribution the probability of  $x$  success in  $N$  experiments can be expressed by the formula:

$$P(x) = \frac{N!}{(N-x)! x!} p^x (1-p)^{N-x}$$

where:

$$\sum_{x=0}^N P(x) = 1,$$

$$\bar{x} = \sum_{x=0}^N x P(x) = pN,$$

$$\sigma^2 \equiv \sum_{x=0}^n (x - \bar{x})^2 P(x) = pn(1-p) = \bar{x}(1-p)$$

$\sigma$  is a dispersion. When  $\bar{x} \gg 1$ , the Poisson distribution can then be approximated by the Gaussian (normal) distribution:

$$P(x) = \frac{1}{\sqrt{2\pi}\sigma} e^{-\frac{(x-\bar{x})^2}{2\sigma^2}}.$$





where  $\sigma^2 = \bar{x}$  is practically a boundary condition. The Gaussian or normal distribution is most often found in the continuous distribution of probabilities of true random  $x$ . In our case the photons fall on the detector. Suppose  $v$  is the average speed of photon detection.  $rdt$  is the differential probability that an event will occur in  $dt$  time, assuming that the photon occurred at time  $t = 0$ . The differential probability that the following photon will occur in  $dt$  time can be calculated by the formula:

$$I_1(t)dt = P(0)rdt,$$

Where  $P(0)$  is the probability of no photon being generated between 0 and  $t$ . It can be expressed by the Poisson distribution:

$$P(0) = \frac{(rt)^0 e^{-rt}}{0!} = e^{-rt}.$$

The differential probability that the following photon will occur in the detector  $dt$  time will be:

$$I_1(t)dt = re^{-rt}dt.$$

Probability of time interval distribution between two subsequent detected photons for different average velocities is shown in Fig. 5.

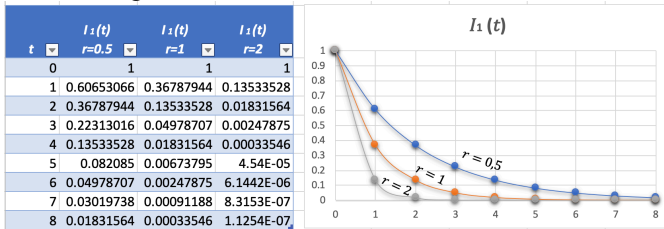


Fig. 5. probability of time interval distribution between two subsequent detected photons for different average velocities.

### 3. Experiment description and conclusion

Fig.6. demonstrates the principal scheme of a phase spectrofluorometer. As a light source we used high-sensitivity impulsive nitrogen laser NL-100 (frequency 0-25 Hz). In order to reduce the "electronic noise" caused by the relaxation processes, we used a multichannel analyzer that is compatible with computer-compatible electronic devices, such as ADC (analog-digital conversion), DAC (digital analog conversion) and electronic circuits.

Fluorescence excitation in phase fluorometers occurs with a light beam that is modulated by high frequency. Fluorescence phase, i.e., the degree of modulation will be compared to the light phase. In the case of exponentially fading fluorescence, the shift  $\psi$  between the fluorescent radiation and excitation light phases is depicted with the expression:  $\omega\tau = tg\psi$ , where  $\tau$  is fluorescence life expectancy, and  $\omega$  is an angular velocity of the modulation. The signal from the source and the fluorescent signal excited on the sample hit the detector that registers the phase shifts among these signals. For example, Bailey and Rolfson measured the phase shifts between these two signals, whereas the two output signals coincide with the phase, the detector registered a minimum signal at the output. There are other methods of measuring the  $\psi$  phase shifts based on the determination of the quantity of these two signals. It is obvious that the longer is the life expectancy of fluorescence, the smaller is the size of its modulation. The quality of modulation ( $m_s$ ) in the light beam and fluorescence signal modulation quality ( $m_f$ ) is associated

with the  $\psi$  phase shifts with the ratio of:  $\frac{m_f}{m_s} = \cos\psi$ . The phase shifts measured by these two methods coincide with each other with great accuracy in the case of exponentially fading fluorescence. The distinction is observed only in case of non-exponential fading of fluorescence. One of the main drawbacks of the phase fluorometer in principle is the difficulty in the interpretation of the results which arise in case of non-exponential fading of the fluorescence, but Birks, Dyson and Munro have used this method even in case of non-exponential fading of the fluorescence. In the first phase fluorometers, polarizing exciting light and Kerr effect were used for light beam modulation. In this case, the high-frequency field acts on the fluid or crystal electronic-optical effect. Then, for light modulation, the light diffraction was studied on the ultrasonic waves in the fluid that formed the quartz crystal. The light beam with the constant intensity falls onto the diffraction grating. Among the easiest methods a high-frequency pipe is used, in which the modular light is obtained directly [17]. A relatively convenient method is to use a hydrogen lamp that is powered by a modulated signal.

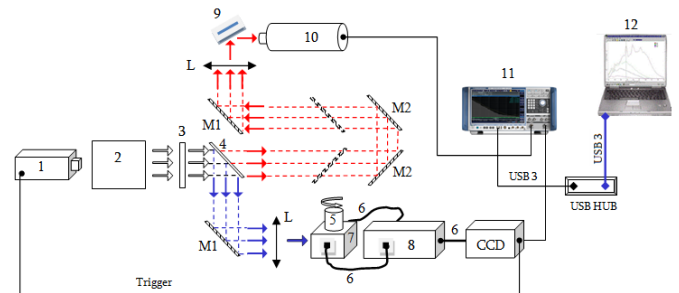


Fig. 6. Principal scheme of phase fluorometer. 1- light source, 2 – optical modulator; 3- optical filter, 4- light splitter; 5 – cuvette with rotation system; 6 – optical fiber; 7 – cuvette holder; 8 – correlator of coherence beams; 9 - scattering plate; 10 - photomultiplier; 11 – phase meter; 12 - computer; M1 – stationary mirror; M2 - moving mirror; L - converging lens; CCD - monochromator.

Thus, the phase fluorometer allows us to determine the duration of the received signal through the phase screen with a well-known modulation signal. It is the iterative methods that have been developed and widely applied in the tasks of synthesis of diffractive optical elements [18]. The main advantage of these methods is that iteration algorithms are more accurate than other algorithms. On the other hand, the realization of the algorithm of synthesis of optical elements on the computer requires significant computing costs. The disadvantage of these algorithms is the use of approximation to describe the laser beam distribution. The lifespan of fluorescence can be determined indirectly, from the attempts of damping fluorescence [19].

It is Important to know the polarization of the source in defining the phase screen regulations (viscosity, temperature, structure) [20].

Fig.7. demonstrates a sample of the 3D spectrum of fluorescence when the excitation wavelength is 200-800 nm, when the fluorescence wavelength is placed in the interval (a) 250-620 nm – short and (b) 620 - 800 nm long wavelengths respectively. As a spectrofluorometer the Black-Comet (190-1100 nm) from company StellarNet was used.



Fluorescence Analysis for Bio-Imaging as a computation demonstration was contributed by: Masato Ohgishi Based on a program by: Shadi Ashnai. This Demonstration is intended to be used for bio- and medical-imaging analysis. The program automatically creates thresholds for the given image, determining the segments of bright fluorescence. Choose a segment and the computer will calculate the size (in pixels), the total fluorescence, and the fluorescence per pixel of the selected segment. On the fig. 8 below calculated "Data List" for segments is shown.

Quantitative characteristics of spectra such as Base, Power Spectral Density (PSD) and Width allow us to collect data that is the basis for capturing high quality three-dimensional spectra. Based on the shape of the spectrum and the tabular data, it is possible to analyze the spectral composition of a bio- and medical-imaging analysis.

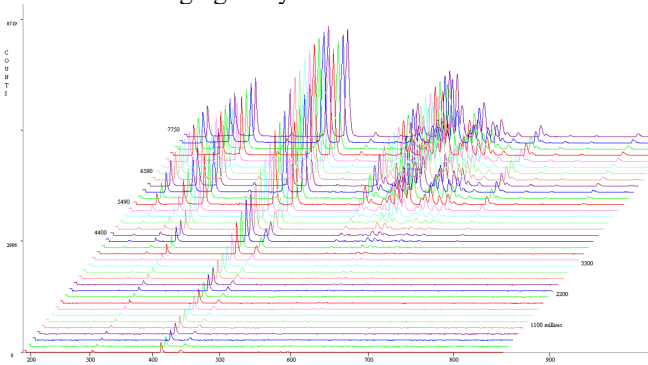
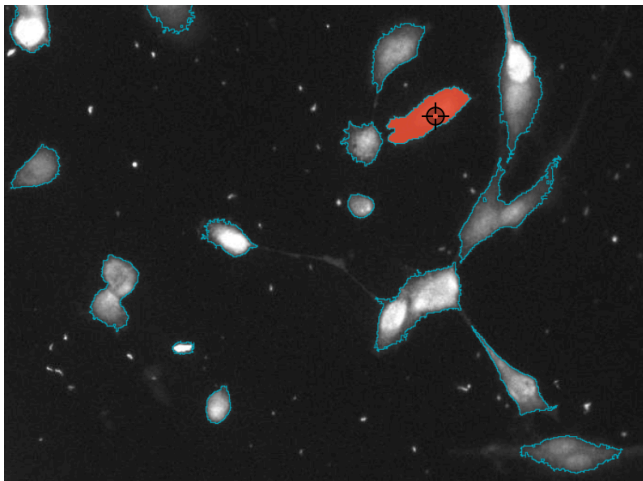


Fig. 7. Sample of the 3D spectrum of fluorescence. The excitation wavelength is 200-800 nm



Segment Number	Area Size	Fluorescence	F/S
1	1873	1287.76	0.687539
2	1193	329.718	0.276377
3	4094	2072.07	0.506125
4	2251	901.235	0.400371
5	2725	1112.61	0.408296
6	1396	596.059	0.426976
7	1527	569.616	0.373029
8	3861	1344.94	0.348339
9	586	269.537	0.459961
10	1380	810.816	0.587548
11	2524	1192.92	0.472631
12	4406	2566.35	0.582466
13	1947	871.596	0.447661
14	272	161.435	0.593512
15	815	436.451	0.535523
16	2719	906.357	0.333342

Fig. 8. Medical-imaging fluorescence analysis for bio-particles and data list for segments

### References

- [1] Turmanidze R. Evaluation of the correlation function of the fluctuation of the laser beam intensity in the blood. Master thesis. Batumi, 2017 (in Georgian)
- [2] Stokes G. G. Über die Veränderung der Brechbarkeit des Lichts, *Annalen der Physik*, B. 163 (11), 1852, S. 480-490
- [3] Berlman I.B. 1971. Handbook of fluorescence spectra of aromatic molecules, 2nd ed. Academic Press, New York.
- [4] Korotkova O., Andrews L.C. "Speckle propagation through atmospheric turbulence: effects of partial coherence of the target", (SPIE pr., 2002)
- [5] Bernard V. Molecular Fluorescence: Principles and Applications. — Wiley-VCH Verlag GmbH, 2001.
- [6] Banakh V. A., Buldakov V.M., Mironov V. L. "Intensity fluctuations of a partially coherent light beam in a turbulent atmosphere", *Opt. Spectrosk.*, 54, 1054-1059 (1983).
- [7] Fante L. "Intensity fluctuations of an optical wave in a turbulent medium, effect of source coherence", *Opt. Acta*, 28, 1203-1207 (1981).
- [8] Gomidze N.Kh, Shashikadze Z.Kh., Makharadze K.A., Khajishvili M.R. About fluorescence excitation spectrums. 6th International Conference on Advanced Optoelectronics and Lasers. Conference Proceedings. 9-13 September (2013), Sudak, Ukraine, pp. 317-319.
- [9] Belenkii M. S., Kon A.I., Mironov V.L. Turbulent distortions of the spatial coherence of a laser beam, *Kvantovaya Electron. (Moscow)*, 4, 517-523 (1977).
- [10] Leader J. C. "Intensity fluctuations resulting from a spatially partially coherent light propagating through atmospheric turbulence", *J. Opt. Soc. Am. A*, Vol.69, 1, 73 – 84 (1979).
- [11] Mandel L., Wolf E. *Optical Coherence and Quantum Optics* (Cambridge University Press, Cambridge, 1995).
- [12] Joseph R. Lakowicz Z. *Principles of Fluorescence Spectroscopy* / R. J. Lakowicz. -N.Y.: Springer Science, 2006. — 960 p.
- [13] Gomidze N.Kh, Shashikadze Z.Kh., Makharadze K.A., Khajishvili M.R. About fluorescence excitation spectrums. 6th International Conference on Advanced Optoelectronics and Lasers. Conference Proceedings. 9-13 September (2013), Sudak, Ukraine, pp. 317-319.
- [14] Gomidze N.Kh., Khajishvili M.R., Makharadze K.A., Jabnidze I.N. , Surmanidze Z.J. About Statistical Moments of Scattered Laser Radiation from Random Phase Screen. *International Journal of Emerging Technology and Advanced Engineering*. ISSN 2250-2459 (ISO 9001:2008 Certified), Vol. 6, Issue 4, pp.237-245, 2016.
- [15] Gomidze N.Kh., Makharadze K.A., Khajishvili M.R., Shashikadze Z.Kh. About Numerical Analyses of Sea Water with Laser Spectroscopy Method. 2011 XXXth URSI General Assembly and Scientific Symposium, 30TH 2011 (5 VOLS), pp. 1620-1624, ISBN 978-1-4244-5117-3.



- [16] Gomidze N., Shainidze J., Shengelia G., Turmanidze R. To the problems of fluorescence excitation spectrums. International scientific journal "machines. Technologies. Materials." web ISSN 1314-507X; print ISSN: 1313-0226, pp.279-282, 2018.
- [17] Misievich S.K., Skidanova R.V. Journal Computer optics and nanophotonics, pp. 269-281, 2017
- [18] Gomidze N. Kh., Khajishvili M. R., Jabnidze I. N., Makharadze K. A., Surmanidze Z. J. To the Problems of Detecting Signals Passing Through a Random Phase Screen. Journal "Recent Advances in Technology Research and Education" Springer International Publishing. Print ISBN: 978-3-319-99833-6, Electronic ISBN: 978-3-319-99834-3, pp. 177-184, 2018.
- [19] Gomidze N., Makharadze K., Jabnidze I., Kalandadze L., Khajishvili M., Nakashidze O. To the Diagnostics of Optically Dense Media via Phase Screen Model. Conference Proceedings. 2019 IEEE 8th International Conference on Advanced Optoelectronics and Lasers (CAOL 2019). IEEE Explore Publisher. ISBN: 978-1-7281-1813-0, pp.71-74, 2019 Google scholar, Scopus, web of science.
- [20] Gomidze N.Kh., Shainidze J.J., Jabnidze I.N., Makharadze K.A., Khajishvili M.R., Kalandadze L.G., Nakashidze O., Mshkhaladze E.N. Estimation of scintillation index for a Gaussian laser beam propagating through a random phase screen. Journal of Biological Physics and Chemistry, Vol. 20 (2020), pp.104-110. doi: 10.4024/27GO19A.jbpc.20.03
- [21] Blinder S.M. Introduction to Quantum Mechanics, Amsterdam: Elsevier, 2004 pp. 68–71.
- [22] Hoppe W., Lohmann W., Markl H., and Ziegler H. Biophysics, New York: Springer-Verlag, 1983.
- [23] Videen G., Ngo D. "Light Scattering from a Cell," in Optics of Biological Particles, NATO Science Series, Series II: Mathematics, Physics and Chemistry, Vol. 238, (A. Hoekstra, V. Maltsev, and G. Videen, eds.), New York: Springer, 2007.

## Nonlinear optical spectroscopy of biointerfaces

C. Humbert

Université Paris-Saclay, CNRS, Institut de Chimie Physique, UMR 8000, 91405 Orsay, France  
[christophe.humbert@universite-paris-saclay.fr](mailto:christophe.humbert@universite-paris-saclay.fr)

**Abstract.** Nonlinear optical spectroscopy allows to probe the physico-chemical properties of (bio)molecular materials at interfaces from nanometer to micrometer scale. Among these, Sum-Frequency Generation (SFG) spectroscopy is an Infrared (IR)-Visible (Vis) vibroelectronic optical probe that can be used for the characterization of the (bio)molecular recognition process in the framework of optical sensors used for instance in medical diagnosis. After a description of the fundamentals of nonlinear optical spectroscopy and its applications to address questions related to biology, specific features of SFG spectroscopy with respect to UV-Visible absorption, fluorescence, Infrared and Raman probes are highlighted through the example of chemical sensors based on metal and semiconducting nanoparticles.

### 1. Introduction

Biointerfaces are complex systems encountered in many fundamental and applied issues related to biological (nano)objects. Due to the overwhelming amount of bulk materials located on each side of these interfaces, classical IR and Raman vibrational spectroscopies do not allow to extract specific information from this thin area of interest. A differential spectroscopic approach is usually performed to overcome this difficulty to distinguish the surface signal from the bulk signal but reveals quickly of limited sensitivity. An alternative dedicated probe based on nonlinear optics is Sum-Frequency Generation (SFG) spectroscopy, used as a complementary technique with respect to the above-mentioned ones. In fact, in biology, the cell membranes act as barriers to: (I) protect the nucleus and organelles from external intrusions; (II) allow matter-energy exchanges necessary to sustain cell-life and reproduction, these transfers being monitored through membrane (channel) proteins located inside lipid bilayers (LB). LB constitute therefore intelligent frontiers between two aqueous media inside a living organism, that should be characterized at the molecular level by surface vibrational spectroscopy [1].

### 2. Methods

SFG spectroscopy is based on a nonlinear coherent second order optical process requiring the use of two incident IR and Vis pulse-shaped laser beams (ps, fs timescale). Both beams

are tuneable in the [2.5-8 $\mu$ m] and [420-700 nm] spectral ranges, respectively. By mixing them on the same point of the probed interface, the latter can generate, due to symmetry breaking of the electronic properties in this special area, a third coherent beam following the energy ( $\omega_{\text{SFG}} = \omega_{\text{Vis}} + \omega_{\text{IR}}$ ) and momentum ( $k_{\parallel, \text{SFG}} = k_{\parallel, \text{Vis}} + k_{\parallel, \text{IR}}$ ) conservation rules. In these conditions, the SFG signal gives access to the nonlinear 2<sup>nd</sup> order susceptibilities ( $\chi_{\text{int}}^{(2)}$ , 3<sup>rd</sup> rank tensor, 27 components) of the probed interface, provided that various polarization schemes are implemented. In classical ps-SFG spectroscopy, the visible wavelength is fixed in the green, while the IR wavelength is changed in order to highlight the vibration modes of molecules localized at the biointerface and its kinetics. In dynamics fs-SFG spectroscopy, one IR pulse encompasses an extended spectral range, allowing to follow in real-time structural changes and reorganization of the biointerface upon external stress [2]. In Two-Colour Sum-frequency generation (2C-SFG) spectroscopy, both IR and visible beams are simultaneously or alternatively tuned in wavelength in order to probe potential vibroelectronic couplings in biointerfaces based on (nano)structured platforms made of semiconducting or metal nanoparticles. Related applications lie for instance in improved biomolecular recognition process in sensors through light amplification of the SFG signal by electronic enhancements mediated by excitons [3] or surface plasmons [4].

### 3. Illustrative results

Biological model membranes (lipid monolayers) built from Langmuir films are extensively studied by SFG in aqueous environments in order to check their structural reorganization under various parameters such as pressure, composition, ionic content, interacting molecules. Besides, in asymmetric LB, when supported on a substrate, it is possible to investigate by SFG the flip-flop mechanism (i.e. the interleaflet displacement in homogeneous LB) and the gel to liquid crystal phase



transition (hybrid LB). Peptides and proteins adsorption in contact with aqueous/liquid or liquid/solid interfaces equally induces their structural conformation as a function of the pH or in contact with biopolymers. Among these, biosensing take a significant place in SFG spectroscopy as illustrated in Figure 1 by the case of the specific biomolecular recognition of avidin by biocytin, without having to use fluorescent or IR markers, contrary to conventional spectroscopies. SFG is a label-free method.

SFG is also used for probing and characterizing the oligonucleotides involved in DNA strands hybridization as a function of the helix direction, showing that this technique is also sensitive to the chirality of complex biological systems. More recently, 2C-SFG revealed successful in enhancing the optical response in QDs-based nanosensors through the highlighting of a dipolar coupling from excitons through their ligands or their close chemical surroundings: this experimental evidence opens the door to enhanced efficient optical characterization by decreasing the manufacturing costs in future applications related to medical diagnosis.

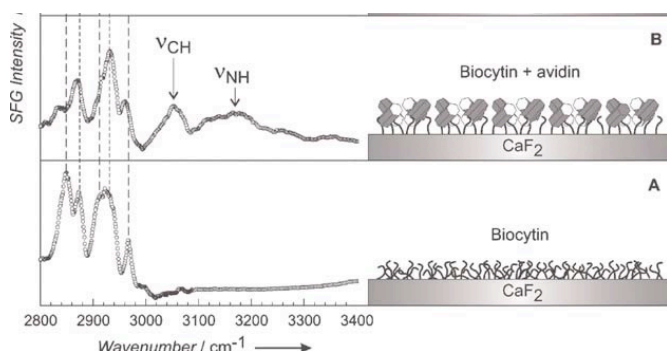


**Figure 1: Biomolecular recognition process by nonlinear optical spectroscopy. SFG spectra of a biocytin monolayer on CaF<sub>2</sub>. (A) bare monolayer; (B) after interaction with avidin. From reference [5]**

## Conclusions

SFG spectroscopy is an advanced optical characterization tool of (nano)materials and (bio)molecules at interfaces for any scale ranging from the atomic to the microscale. It is now commonly exploited by the community of physicists and chemists worldwide for many applications. The biology frontier has been crossed these last years by this technique, giving access to original specific information in complex system from small peptides to DNA strands on nanostructured platforms as it is under intensive developments.

## References

- [1] Humbert C., Busson B., Sum-frequency generation spectroscopy of biointerfaces, in *Biointerfaces characterization by Advanced IR spectroscopy*, 2011, Elsevier, pp.279-321.
- [2] Hosseinpour S., Roeters S. J., Bonn M., Peukert W., Woutersen S., Weidner T. Structure and Dynamics of Interfacial Peptides and Proteins from Vibrational Sum-Frequency Generation Spectroscopy, *Chem. Rev.*, 2020, 120, 3420-3465.
- [3] Noblet T., Boujday S., Méthivier C., Busson B., Tadjeddine A., Humbert, C., Semiconductor quantum dots reveal dipolar coupling from exciton to ligand vibration, *Comm. Chem.*, 2018, 1, 76.
- [4] Dalstein L., Humbert C., Ben Haddada M., Boujday S., Barbillon G., Busson B., The Prevailing Role of Hotspots in Plasmon-Enhanced Sum-Frequency Generation Spectroscopy, *J. Phys. Chem. Lett.*, 2019, 10, 7706-7711.
- [5] Dreesen L., Sartenaer Y., Humbert C., Mani A.A., Méthivier C., Pradier C.-M., Thiry P.A., Peremans A., *ChemPhysChem*, 2004, 5, 1719.

# Nanotechnology in the applied medicine – current trends and innovations

L. Sajti

<sup>1</sup> AIT Austrian Institute of Technology and RHP Technology, Viktor-Kaplan-Str. 2, 2700 Wiener Neustadt, Austria  
[L.Sa@rhp.at](mailto:L.Sa@rhp.at)

**Abstract.** Significant improvements of state-of-the-art, osteo-anchored implants (e.g. dental implants, endoprosthesis, etc.) as well as 3D-printed ceramic and polymeric biomaterials are considered. The correlation of non-optimized implant surfaces and inflammatory cell-material interactions are discussed in detail. Based on nanotechnology-based innovations the aim is to develop novel material solutions for a broad range of medical applications and improving the patient experience (decrease severe pain, further surgical interventions, explantation or re-implantation procedures). The development of highly biocompatible permanent and biodegradable implant materials, additives and coatings are highlighted allowing a long-term biofunctionalization of metallic, ceramic and polymeric biomaterials. Achievement of long-term and local antibacterial, anti-thrombotic, osseointegrative or anti-inflammatory behaviours are discussed in detail. With the combination of relevant biological functions, material integration into the surrounding tissues can be accelerated and resulting in biomaterials that are not recognized by the body as artificial materials.

## 1. Introduction

In Europe, 25% of the population is already aged 60 years or over, according to the UN population statistics (The World Population Prospects: The 2017 Revision). That proportion is

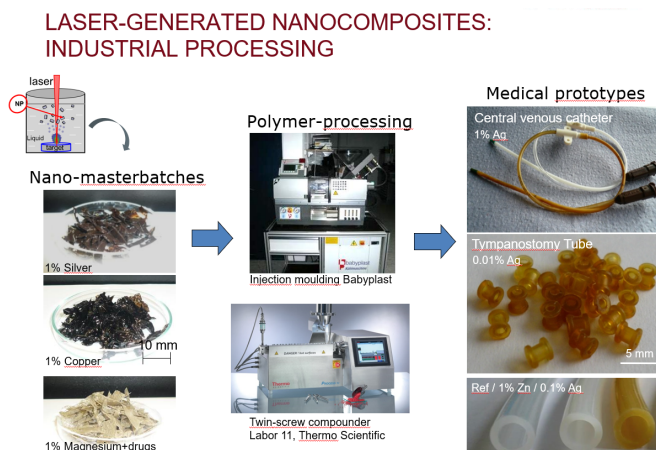
projected to reach 35% in 2050. At the same time, in all age groups, there is a changing trend in less physical activities and unhealthier lifestyles, which will result in an enhancing percentage in obesity, allergies and chronic diseases. This will apply an enormous pressure on the health and biomedical sector, which is therefore on a massive growth path. Besides orthopedic, trauma and craniomaxillofacial implants (screws, plates, fixations) especially for high-risk sport injuries, the elderly-aged group will have an increasing demand for reconstruction of joints (hip, knee, shoulder) as well as for coronary and peripheral stents or vascular grafts. In the following years, this will trigger a huge demand from the medical industry to develop biomaterials with superior material properties and innovative features. The main request for the new generation of biomaterials is a long-term protection against infections, thrombosis as well inflammatory cell reactions that are crucial factors for a sufficient material integration into the surrounding tissue. Therefore, there is a



need for biofunctionalized materials and coatings for medical implants in order to avoid or at least significantly to reduce these processes.

## 2. Method and approach

In contrast to the established implant surface technologies, we highlight the innovative approach of ultra-pure nanoparticle-based implant coatings and additives as long-term bioactive interfaces facilitating tissue integration for various implant types. A high-power laser system is used allowing the synthesis of ultra-pure nanocolloids based on metallic and stoichiometric alloys via liquid phase laser ablation. These colloids are used for antibacterial or cell-proliferative coatings and additives based on silver, gold, copper or platinum as raw material, using standard industrial coating methods such as spray-, plasma- or ultrasound coating to apply these nanocolloids on the surfaces of implants. To cover polymer implant applications, laser ablation in organic monomers and solvents are applied for the direct doping of the polymer matrix with the relevant nanoparticles without modifying the starting organic surrounding. This opens a completely new perspective for polymeric implants with industrial processability (e.g. extrusion, injection moulding) for a broad range of medical implants.



For 3D-printable and sinterable bioactive material the laser-synthesized nanoparticle are deposited on industrially-relevant microparticle host without any chemical modification leading to an innovative nanocomposite that provides biologically active characteristics and industrial processability. In this paper a nanoparticle-modified  $\beta$ -tricalcium phosphate system is described as relevant material for instance for the treatment of cranial defects.

For the production of metallic implant raw materials with enhanced mechanical characteristics, equal channel angular pressing (ECAP) is used shown in Fig. 1. The method results in optimized material performance such as high-strength, high ductility, high hardness as relevant measures for the treatment of critical bone defects during trauma and reconstruction surgery.

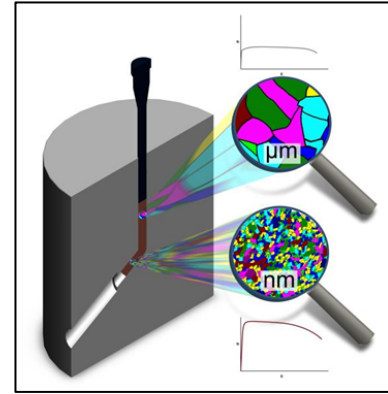


Fig. 1. Schematic image of the ECAP process

## 3. Illustrative results

Laser-generated ultrapure, metallic nanoparticles are highly stable due to process-related charged elements and therefore can be used as coating elements and deposited with a wide variety of methods including electrophoretic deposition shown in Fig. 2. for the application of neuronal electrodes.

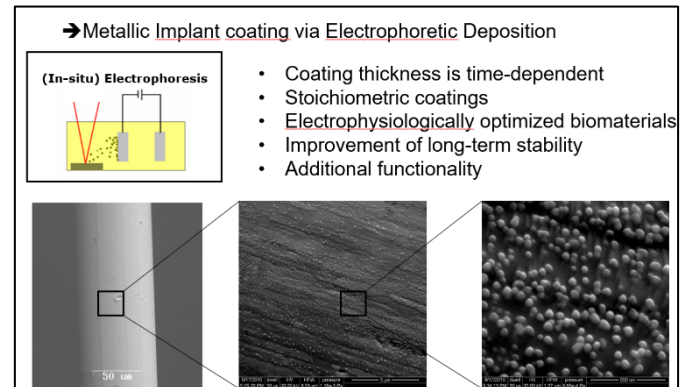
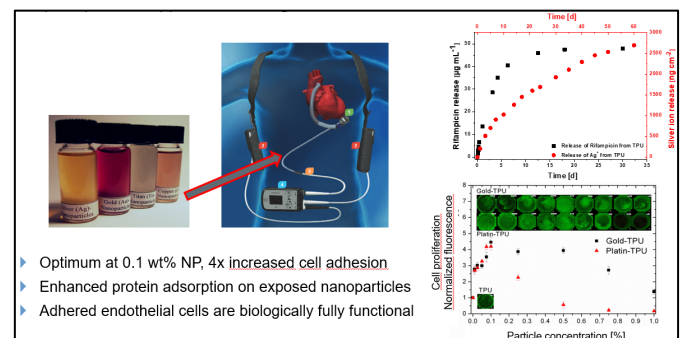


Figure 2. Electrophoretic coating of a PtIr mid-brain implant with laser-generated stoichiometric PtIr-nanoparticles.

In order to improve the long-term infection control on the surface of a Left Ventricular Assist Device (LVAD) – the embedding of silver nanoparticle has been realized into a thermoplastic polyurethane catheter, coated with gold-nanoparticle and an organic drug. The as generated complex implant surface allows a short-term burst release of a strong antibiotic (Rifampicin) combined with a mild antimicrobial potential based on the release of silver-ions. Finally the additional noble metal coating results in a fast wound healing process combined with antithrombotic behaviour, presented in Fig. 3.





**Figure 3. Complex surface characteristic of an artificial heart device with short and long-term antibacterial protection combined with long-term antithrombotic behaviour.**

Surface functionalization of various material classes included metallic, ceramic and polymeric was achieved using ultrapure, laser-generated nanoparticles as active surface components using industrially relevant processing technologies. High temperature sinterable ceramic composites were developed for the treatment of bone defects. Critical combination of local antibacterial efficacy with improved cell-growth of osteoblasts were achieved via the combination of locally antimicrobial and cell-proliferative particles such as silver and gold, respectively. The as synthesized composites could be sintered up to 1100 °C without losing the biological potential of the nanoparticle-coating (Fig. 4, left). Covalently bonded bioactive coatings were realized on central venous catheter surfaces (Fig. 4, middle) while a nanoparticle-coating was realized on a Ti64 hip-implant material via spray and plasma-coating (Fig. 4, right). The next innovation step is the combination of the various biological features following by the necessary pre-clinical and clinical evaluations.

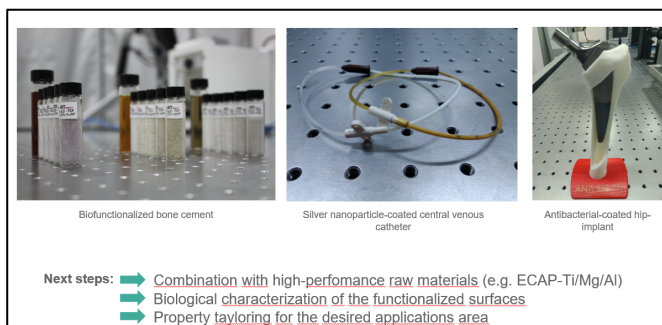


**Figure 4. Ultrapure nanoparticle coatings on various biomaterial surfaces.**

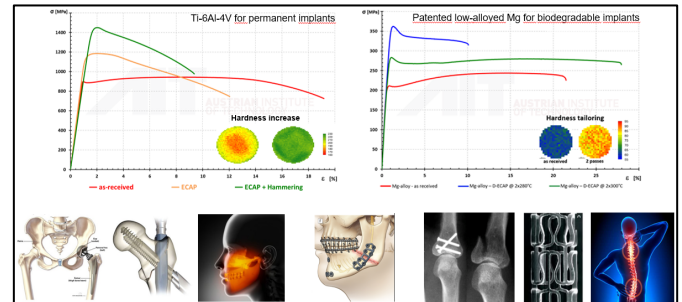


**Figure 5. Mechanical characteristics of ECAP-processed biomaterials and corresponding fields of applications.**

Finally, ECAP-treated permanent and biodegradable materials was highlighted showing optimized mechanical performances (Fig. 5). In case of a medically relevant Ti-alloy, a 50 % increase in material strength and a 40 % increase in hardness was achieved. During the ECAP-treatment of a patented Mg-alloy besides the improvement of strength and hardness and increased elongation could be achieved that is relevant for high-deformation application (e.g. cardiovascular stents).

### Conclusions

Laser-generated ultrapure nanoparticles are presented for a wide range of medical applications. Critical material performances such as long-term antibacterial and antithrombotic behaviour were improved using various industrially relevant processing technologies such as extrusion, injection moulding, ultrasound spray, plasma-coating besides many others. Finally, equal channel angular pressing has been presented allowing the improvement of vital material characteristics of metallic biomaterials without changing the cross-sectional area of the biomaterials. Data analysis revealed the strong dependence of processing conditions and the final mechanical characteristics allowing to precisely tailor the material performance regarding the actual medical application. Signature of bio-particles of a given parameters is proposed for consideration.

## 3D Printing and 3D Scanning: Applications in the Cultural Heritage field

A. Kantaros<sup>1,a</sup>, T. Ganetsos<sup>1,b</sup>, D. Tseles<sup>1,c</sup>

<sup>1</sup> Department of Industrial Design and Production Engineering, University of West Attica, 12244 Athens, Greece.

<sup>a</sup> [akantaros@uniwa.gr](mailto:akantaros@uniwa.gr), <sup>b</sup> [ganetsos@uniwa.gr](mailto:ganetsos@uniwa.gr), <sup>c</sup> [dtsel@uniwa.gr](mailto:dtsel@uniwa.gr)

**Abstract.** In the last decade, the introduction of desktop 3D Printers and 3D Scanners led to their use in a vast array of application. Their portability and interconnectivity enabled users to use such technologies in-situ for better results. Desktop 3D Printing techniques range from the use of thermoplastic to liquid photocurable resins as raw materials, while desktop 3D Scanners use methods such as laser and structured light in order to achieve optimum results. Such technologies can be integrated to existing techniques used in the cultural heritage restoration and preservation field and assist towards achieving better and faster results in relevant operations.

### 1. Introduction

In the last years, the continuous evolution of 3D imaging and fabrication technologies (3D Scanning and 3D Printing respectively) has led to numerous novel applications in a

number of scientific fields. The field of Cultural Heritage is, undoubtedly, one such sector where the potential of the aforementioned technologies has started to make an impact. In this context, 3D Scanning technology offers the ability to digitize artefacts and archaeological materials serving the dual purpose of digital preservation and on the other hand to reveal a great degree of crucial details that are unrecognizable with the bare eye. Also, by employing 3D Printing Technology in the Cultural Heritage field, conservators and archaeologists can benefit from fabricating precise, highly detailed, replicas of separate components or the whole artifact. Fabricating an exact replica of an artifact, especially when certain



components are missing, can help conservators and archaeologists to compile a complete reconstruction.

with a EinScan Pro 2X Plus (Shining 3D Tech. Co., Ltd.) using Shining Software as depicted in figure 1.

## 2. Method and approach

The use of price-effective, commercially available 3D Scanners and 3D Printers, that are portable and can be used in the field [3], in order to test the quality and speed of reproduction and its applicability to hands-on education and artifact dissemination purposes. Authors aim to establish an optimised procedure workflow that will lead to the rapid and qualitative exploitation of the aforementioned equipment.

## 3. Results

The first case [1] has to do with the Limestone Sculptures known as “The Kouroi of Atalanti” which were 3D scanned

The second case [2] has to do with a Homo naledi cranium which was obtained from an excavation site, was 3D scanned and a scaled-down replica was 3D printed as shown in figure 2.



Fig. 1 Results of 3D scanning in natural size kouros



Fig. 2. Experimental setup used to measure the cranium in 3D and Homo naledi cranium (left) and 3D printed replica of skull as it was removed from the 3D printer (right)

The third case has to do with measurements in an excavation site in Delphi, Greece, where in cooperation with conservators and archaeologists, 3D Scanning in findings and artisans is performed along with 3D Printing in order to produce exact replicas.

## Conclusions

The aforementioned case studies prove that the employment of portable 3D Scanning and 3D Printing equipment has great potential and can produce results of high scientific value in the Cultural Heritage restoration and preservation field. Not only the portable 3D Printing and 3D Scanning equipment proved capable to fulfil the required tasks, but an optimized procedure workflow that will lead a more rapid use of these technology is the goal of our team's future work.

## References

- [1] Maria I. Papageorgiou, Theodore Ganetsos, The “Kouroi of Atalanti”: Limestone Funerary Statues and Grave Stele from the Cemetery of Ancient Opous (Atalanti): Preliminary Study, Analysis and Investigation of the Composition, Variety and Possible Sources of Limestone of a New Locrian Sculpture Workshop, *Archaeology*, Vol. 9 No. 1, 2021, pp. 41-46. doi: 10.5923/j.archaeology.20210901.08.
- [2] Konstantinos Naseb, Petros I. Stavroulakis, Karim Sadr, Theodore Ganetsos, Nikolaos Laskaris, Digital 3D Preservation of a Rare Homo Naledi Skull, *Archaeology*, Vol. 9 No. 1, 2021, pp. 54-55. doi: 10.5923/j.archaeology.20210901.10.
- [3] Kantaros Antreas, Dimitrios Piromalis, Employing a Low-Cost Desktop 3D Printer: Challenges, and How to Overcome Them by Tuning Key Process Parameters, *International Journal of Mechanics and Applications*, Vol. 10 No. 1, 2021, pp. 11-19. doi: 10.5923/j.mechanics.20211001.02.

